Lehigh University
Lehigh Preserve

Theses and Dissertations

1994

Potential for high-performance steel in a long span truss bridge

Zhihong Li
Lehigh University

Follow this and additional works at: http://preserve.lehigh.edu/etd

Recommended Citation
Li, Zhihong, "Potential for high-performance steel in a long span truss bridge" (1994). *Theses and Dissertations.* Paper 314.

This Thesis is brought to you for free and open access by Lehigh Preserve. It has been accepted for inclusion in Theses and Dissertations by an authorized administrator of Lehigh Preserve. For more information, please contact preserve@lehigh.edu.

AUTHOR:

Li, Zhihong

TITLE:

Potential for High-Performance Steel in a Long Span Truss Bridge

DATE: October 9, 1994

Potential for High-Performance Steel in a Long Span Truss Bridge

by

Zhihong Li

A Thesis
Presented to the Graduate and Research Committee
of Lehigh University
in Candidacy for the Degree of
Master of Science

in

Civil Engineering

Lehigh University
Bethlehem, Pennsylvania

August 1994

This thesis is accepted and approved in partial fulfillment of the requirements for the degree of Master of Science in Civil Engineering.

August 25, 1994
Date

Dr. Richard Sause
Advisor

Dr. Le-Wu Lu
Chairman
Department of Civil Engineering

ACKNOWLEDGEMENT

The research presented herein was conducted at the ATLSS Center of Lehigh University. The patient help and guidance of Dr. Richard Sause, the thesis supervisor, is greatly appreciated. I acknowledge my gratitude to Dr. John Kulicki, Dr. Wagdy Wassef and Mr. Eugene Waldner of Modjeski & Masters, Inc. for providing the original design of the Greater New Orleans Bridge #2 and for many helpful discussions on the use of the AASHTO LRFD code and on truss bridge design. Special thanks are due to Dr. John W. Fisher, Director of the ATLSS Center, for his suggestions on fatigue design.

ABSTRACT

The potential for high-performance steel in a long span truss bridge is investigated by conducting a comparative design study. High-performance steels (HPS) are steels with high strength, high fracture toughness, good weldability, and other desirable properties. Since yield strength is the primary property of steel considered in bridge design codes, this investigation focused on HPS with a range of yield strengths. Optimum designs using steels with yield strengths ranging from 36 ksi (248 Mpa) to 120 ksi (827 Mpa) are investigated for three member types in the Greater New Orleans Bridge #2: rolled-shape stringers, welded floor beams, and box-shape truss members. The results indicate that: (1) using current bridge configurations and design codes, weight reduction with increasing yield strength in stringers is possible for steels with yield strengths from 36 ksi (248 Mpa) to 70 ksi (483 Mpa), however, above 70 ksi (483 Mpa), fatigue at the stringer-diaphragm connection prevents further weight reduction; (2) in floor beams, the potential for HPS can be fully utilized, resulting in weight reduction with increasing yield strength for the range of yield strengths considered; (3) in tension truss members, member weight decreases in proportion with increasing steel yield strength, however, in compression truss members, the decrease in weight that can be achieved depends on the axial force level, and the decrease in weight with increasing yield strength is larger for members with larger axial forces.

Table of Contents

List of Tables

List of Figures

Chapter 1 Introduction

1.1 Background

This study is part of a Federal Highway Administration (FHWA) sponsored project "Innovative Bridge Designs Using Enhanced Performance Steels". The objective of the project is to determine the feasibility for using high-performance steel (HPS) in highway bridges. The initial stage of the project focuses on the potential for utilizing HPS in present-day bridge designs. The second stage focuses on new bridge forms which may make even more effective use of HPS. The present study is part of the first stage of the project.

Participants in the project are: (1) Modjeski and Masters, Inc., a bridge consulting engineering firm located in Harrisburg, Pennsylvania; (2) the Engineering Research Center for Advanced Technology for Large Structural Systems (ATLSS) at Lehigh University; and (3) the University of Michigan.

1.2 Objective and Scope

The objective of this study is to determine the feasibility of using high-performance steel in a long span truss bridge, the Greater New Orleans Bridge #2, within the framework of the recently developed AASHTO LRFD design standards [AASHTO, 1993]. The strength, service, and fatigue limit states of the LRFD code are considered in the study.

High-performance steels are steels made using advanced compositions and/or

processing practices that provide the steel with improved properties, such as high strength, high fracture toughness, good weldability and other desirable properties, which are important in highway bridge designs. This study considers high strength, high performance steels with low carbon and carbon equivalent which provides good weldability ([Graville, 1976]). Since yield strength is the primary property of steel considered in bridge design specifications, it is the primary property of HPS discussed in this study. The yield strength range investigated in this study is 36 ksi (248 Mpa) to 120 ksi (827 Mpa). Other properties of HPS which might influence the potential for these steels were not considered.

1.3 Approach

To determine the potential for using HPS in bridge designs, a comparative design study for a specific bridge was conducted. The Greater New Orleans Bridge #2 was selected for this purpose. By redesigning the bridge in HPS and comparing the redesigns with designs in conventional steel, the potential for HPS was evaluated. Because of the uncertainties and complexities involved in the process of fabrication, erection, and maintenance, only the material weight is considered.

It is recognized that the market for HPS will be in bridges of the future, therefore the recently approved AASHTO LRFD code [AASHTO 1993] is adopted in the redesign of the bridge. The existing design of the bridge, furnished by Modjeski & Masters, Inc., was based on an earlier version of the AASHTO code. The existing design and the redesigns are not directly comparable. However some comparisons are made, and a few

comparisons between the requirements of the earlier code and the LRFD code are also made.

1.4 Outline of the Thesis

The thesis is organized as follows. A brief review of the AASHTO LRFD code is presented in Chapter 2. Chapter 3 is an introduction to the redesign of the Greater New Orleans Bridge #2. Chapters 4, 5 and 6 discusses the potential for HPS in stringers, floor beams, and truss members of this bridge. Conclusions and limitations of the redesign study as well as recommendations for future studies are included in Chapter 7.

Chapter 2 Review of AASHTO LRFD Code

2.1 Philosophy

The LRFD design philosophy is expressed in equation (2.1-1):

$$\eta\Sigma\gamma_i Q_i \leq \phi R_n = R_r \qquad (2.1\text{-}1)$$

for which:

$$\eta = \eta_D \eta_R \eta_I \qquad (2.1\text{-}2)$$

where,

η_D = a factor relating to ductility (Table 2.1-1)

η_R = a factor relating to redundancy (Table 2.1-1)

η_I = a factor relating to operational importance (Table 2.1-1)

γ_i = load factor

Q_i = force effect

ϕ = resistance factor

R_n = nominal resistance

R_r = factored resistance

Equation (2.1-1) should be satisfied for the four types of limit states specified in the LRFD code: strength limit states, service limit states, fatigue limit states, and extreme event limit states. In this study, it is assumed that the extreme event limit states do not control the design. Only the other three types of limit states are considered.

2.2 Load Combinations

The LRFD code specifies that a certain combination of load effects, due to certain specified types of loads, should be considered for each limit state. Within each load combination, specified load factors are applied to the load effects for each type of load. For the redesign of Greater New Orleans Bridge #2, the following load combinations were considered for the strength, service and fatigue limit states of the bridge:

Strength I Basic load combination related to the normal vehicular use of the bridge

Service II Load combination intended to control yielding of steel structures and slip of slip-critical connections due to vehicular live load

Fatigue Fatigue and fracture load combination relating to repetitive gravitational vehicular live load and dynamic responses under a fatigue design truck.

Table 2.2-1 lists the load factors for the above three load combinations. From its definition, it can be seen that the *Service II* load combination is different from the traditional live load elastic *deflection criteria.* If the load factor concept is applied to the elastic *deflection criteria*, the load factors are 0.0 for dead load and 1.0 for live load. In comparison, for the *Service II* load combination, the load factors are 1.0 for dead load and 1.3 for live load. The purpose of these two service limit states are different. The Service II load combination is intended to prevent permanent deformation under service conditions, while the elastic deflection criteria is to avoid undesirable structural or psychological effects due to live load deflections. As discussed in Section 2.3.1, the live loads for the Service II load combination and the elastic deflection criteria are also different. In LRFD specification, the use of the elastic deflection criteria is optional.

2.3 Live Load Model

2.3.1 Vehicular Live Load

Strength Limit State and Service Limit State For the strength and service limit states, three types of live loads are specified for a typical design lane, as shown in Fig. 2.3-1: a design lane load, a design truck and a design tandem. Note that the spacing between the 32.0 kip (142.34 KN) axles of the design truck should be varied between 14.0 ft (4.27 m) and 30.0 ft (9.14 m) to produce the maximum force effects. Based on the three vehicular live loads, the extreme force effect is taken as the larger of the following:

(1) the effect of the design tandem combined with the effect of the design lane load;

(2) the effect of the design truck combined with the effect of the design lane load;

(3) for negative moment between points of dead load contraflexure, 90% of the effect of two design trucks with a minimum headway distance of 50.0 ft (15.24 m) and the distance between the 32.0 kip (142.34 KN) axles taken as 14.0 ft (4.27 m) combined with 90% of the effect of the design lane load.

For the optional live load elastic *deflection criteria*, the deflection should be taken as the larger value produced by :

(1) the design truck alone, or

(2) the design lane load and 25% of the design truck

Fatigue Limit State For the fatigue limit state, a single fatigue truck is considered regardless of the number of design lanes of the bridge. The fatigue truck is the design truck with a constant spacing of 30.0 ft (9.14 m) between the 32.0 kip (142.34 KN) axles.

2.3.2 Multiple Presence of Live Load

For bridges with multiple design lanes, the LRFD code requires that the bridge be analyzed for cases with different numbers of lanes loaded. As shown in Table 2.3-1, when more lanes are loaded, the loads are scaled down by the so-called multiple presence factors, and when fewer lanes are loaded, the loads are scaled up. Two lanes loaded is the standard case.

2.3.3 Dynamic Load Allowance

Dynamic load allowance is considered by applying a dynamic load allowance or impact factor (IM), as expressed in Equation (2.3-1).

$$\text{dynamic load effect} = (1 + IM) \times \text{static load effect} \qquad (2.3\text{-}1)$$

Specific values of impact factors from the LRFD code are listed in Table 2.3-2. LRFD specifies that the impact factor is applied to the design truck or design tandem loads but not to the design lane load.

2.4 Live Load Distribution

To distribute the live loads specified for each design lane to a typical girder in a multi-girder bridge, approximate load distribution factors are provided by the code. In earlier versions of the AASHTO code [e.g., AASHTO 1989], live load distribution factors have a simple approximate form of S/D, where S is the spacing between longitudinal girders or stringers, and D is a constant determined by the type of bridge and the number of lanes of traffic. The LRFD code (AASHTO 1993) includes a set of more complicated

equations to approximate the distribution of live load between parallel girders of multi-girder bridges. In the redesigns of the Greater New Orleans Bridge #2, the distribution factors for a *Concrete Deck on Steel Beams* bridge type are used for the stringer design. The equations for calculating the distribution factors are included in Table 2.4-1. It should be noted that, the distribution factors in the LRFD code are applied to all of the live loads for one lane, not to the wheel loads as specified in earlier versions of the AASHTO code.

2.5 Load Induced Fatigue design

In LRFD, fatigue is categorized as *load induced* or *distortion induced* fatigue. For *load induced* fatigue design of a steel bridge detail, the force effect is the live load stress range due to the fatigue truck.

Each detail should satisfy equation (2.5-1):

$$\gamma\,(\Delta f)_n \le (\Delta F)_n \qquad (2.5\text{-}1)$$

where,

γ = load factor, taken as 0.75 for the fatigue load combination

$(\Delta f)_n$ = the force effect due to the passage of the fatigue truck

$(\Delta F)_n$ = the nominal fatigue resistance

Chapter 3 Introduction to Redesign of Greater New Orleans Bridge #2

3.1 Member Types in Redesign

Greater New Orleans Bridge #2 is a cantilever through-truss bridge with three spans of 853 ft (260.00 m), 1574 ft (479.76 m) and 590 ft (179.83 m). Fig. 3.1-1 shows the elevation of the bridge. The middle 689 ft (210.01 m) of the center span is constructed as a suspended span, which is simply supported on the cantilevers from the piers. In this study, effort is focused on the redesign of the suspended span. A typical cross section of the suspended span is given in Fig. 3.1-2. It is noted that this bridge provides three member types in which the potential for HPS can be investigated:

Stringers	-	Designed as rolled shapes
Floor beams	-	Designed as welded I beams
Truss Members	-	Designed as built up box members

The three chapters that follow deal with the potential for high-performance steel in each of these three member types.

3.2 Change of Traffic Pattern

The existing Greater New Orleans Bridge #2 was designed for four lanes of regular highway traffic and two lanes of transit rail traffic as shown in Fig 3.2-1. The total roadway width is 94 ft (28.65 m). To simplify the redesign of this bridge, only highway traffic is considered. In addition, the current configuration of the truss members of the bridge is maintained. However, as discussed in Chapter 4 and Chapter 5, the

arrangement of stringers and the configuration of floor beams are modified. Within the roadway width of 94 ft (28.65 m), the bridge is capable of holding seven highway traffic design lanes. In actual use, the bridge is likely to be used for up to six lanes of traffic.

Chapter 4 Potential for High-Performance Steel in Stringers

4.1 Introduction

Stringers are longitudinal members carrying that carry load from the deck to the floor beams. The purpose of this chapter is to investigate the potential for HPS in the stringers of the Greater New Orleans Bridge #2.

Stringers used in this bridge are fabricated from rolled W-shape beams. Since only a limited number of discrete shapes are available, the process of stringer design is quite simple: a minimum weight design can be found by eliminating the inadequate shapes from a small group of candidate shapes. The yield strength levels of rolled shapes are limited by production capabilities of steel makers. In the United States, steel makers supply rolled shapes with yield strengths up to 65 ksi (448 Mpa). In Europe, rolled shapes with yield strength greater than 65 ksi (448 Mpa) are available. In this study, stringers with yield strengths of 36 ksi (248 Mpa), 50 ksi (345 Mpa), 70 ksi (483 Mpa) and 85 ksi (586 Mpa) are considered.

The following limit states of the AASHTO LRFD specification are considered in the redesign of the stringers: strength limit states, service limit states, and fatigue limit states.

4.2 Existing Stringer Design

Fig. 4.2-1 shows the layout of stringers in the existing Greater New Orleans Bridge #2. Stringers in the transit rail part of the roadway are the same as those in the highway part with a smaller spacing due to the heavier transit vehicular load. In the longitudinal

highway part with a smaller spacing due to the heavier transit vehicular load. In the longitudinal direction, stringers rest on floor beams and are continuous over either three spans or four spans. The span length is equal to the floor beam spacing, i.e., the truss panel length, as shown in Fig. 4.2-1. At midspan, a diaphragm frames into the stringer through a gusset plate connected to the web of the stringer by fillet weld. The detail is illustrated in Fig. 4.2-2. In the AASHTO specification, this is a Category C' detail for fatigue design.

For the existing design, the stringer cross section is W33X118, A36 steel in the suspended span.

4.3 Layout of Stringers in Redesign

For highway traffic only, as considered in the redesign, an equal spacing of 7'-1'' is maintained between stringers. This distance is equal to the stringer spacing in the highway part of the roadway of the existing bridge. Since the live load distribution factor for stringers is mainly determined by stringer spacing, the distribution factor in the redesign of stringers 0.651 (based on the LRFD) is close to that of the existing design 0.644 (based on earlier version of the AASHTO code, [e.g., AASHTO 1989]). Fig. 4.3-1 shows the layout of stringers in redesign.

4.4 Stringer Analysis

4.4.1 Analysis Tool

A girder analysis program was developed to perform the stringer analysis. The

program provides moment and shear envelopes based on the LRFD load model for a girder or stringer under the *strength, service*, and *fatigue* limit states. Results are based on a discretized girder analysis model specified by the user. For the stringer analysis, each span of the girder was divided into 10 equal segments.

4.4.2 Analysis Model

The parallel stringer system, comprised of the stringers and concrete deck, is modeled as a continuous parallel girder bridge supported by floor beams, which are assumed to be nondeflecting. The span length of this continuous girder bridge is equal to the spacing of floor beams, and the number of spans is the number of spans over which the stringers are continuous. Corresponding to the two types of stringers used in the Greater New Orleans Bridge #2, two types of continuous girder bridges were analyzed, that is, three-span and four-span. Fig. 4.4-1 shows the three-span continuous model. Each stringer is treated as a one-dimensional girder, which is isolated from the rest of the structure. The cross section of the stringer and the discretized analysis model of the three-span continuous stringers used in the girder analysis program are shown in Fig. 4.4-2.

4.4.3 Design Load

For the strength limit state and the service limit state, dead load and live load are considered. For fatigue limit state, only the fatigue live load is considered. Fig. 4.4-3 shows a discretized three-span continuous girder subjected to the LRFD live load combination for one lane. Live load applied to one girder consists of the live load for one

lane, multiplied by the distribution factor.

For the strength limit state and the service limit state, the three live load combinations in Fig. 4.4-3 (a) are considered, however, the two truck and lane load combination is applied only to negative moment regions between dead load contraflexure points, as illustrated in Fig. 4.4-4 for a three-span continuous stringer. For the fatigue limit state, the design live load is the fatigue truck. It should be pointed out that the distribution factor for fatigue design is the distribution factor for the one-lane-loaded case (see Table 2.4-1) divided by the multiple presence factor 1.20 for the one-lane-loaded case, because this multiple presence factor is already incorporated in the distribution factor formula, and should not be applied to the fatigue truck.

4.5 Redesign of Stringers

4.5.1 General

In the existing bridge, stringers are designed as non-composite sections. The redesign also treats the stringers as non-composite. Table 4.5-1 compares the maximum design moment and shear for the three span and four span continuous stringers. It is found that the differences are very small and the three span continuous stringer is usually subjected to more demanding load effects. Therefore, in this study, effort is concentrated on redesign of three span continuous stringers. Factored and distributed stringer moment and shear envelopes for the strength limit state are given in Fig. 4.5-1 and Fig. 4.5-2.

4.5.2 Critical Load Cases for Negative Bending Moment

Design of the stringers for bending moment considers both positive and negative flexure. The unbraced length is needed to determine the moment resistance of a stringer cross section. Under positive bending moment, the concrete serves as continuous bracing and the unbraced length is zero. Therefore, the moment resistance of a cross section can be determined by the steel yield strength and the dimensions of the section. Depending on the compactness of the rolled shape, the plastic moment or elastic moment resistance is used. The maximum value in the positive moment envelope can be directly taken as the design moment for the positive bending moment calculation.

For negative bending the stringer is not continuously braced so the design is more complicated. In general, bracing is provided by floor beams and diaphragms, however, in some cases, moment contraflexure points in a moment diagram can be included as effective bracing points. Thus, the unbraced length depends on the moment diagram, not the moment envelope. Since the diaphragms are only at the midspan, the unbraced length of a stringer can be as long as half of the span length. In this situation, it is possible that the negative moment resistance of the stringer will be controlled by lateral torsional buckling. The Cb factor used in calculating the moment resistance, as controlled by lateral torsional buckling, depends on the moment values at the two ends of the unbraced portion of the stringer.

Thus to design for negative bending moment, *moment diagrams* of the stringer under critical load cases are needed rather than the negative *moment envelope*. The negative moment envelope gives the possible maximum negative moment for each cross

section of the stringer. However, these maximum values may not occur under the same load case. Therefore, it is necessary to study the corresponding load cases for values on the negative moment envelope, and then calculate the moment diagram for the most critical load cases so that the negative moment resistance capacity of the stringer can be determined and compared with the maximum negative bending moment produced by that particular load case. One of the useful capabilities of the girder analysis program is that it gives the type and position of live load for each moment or shear envelope value. For the negative moment envelope, this information is listed in Table 4.5-2. To make it easier to visualize the results in this table, moment influence lines for several positions along the stringer are given in Fig. 4.5-3.

Table 4.5-2 shows that starting at a certain distance away from the interior supports, the maximum negative moment for different cross sections are produced by the same load cases. In this particular bridge, for the 15 cross sections in one half of the symmetric discretized stringer analysis model, there are 7 unique load cases to be considered. Among them, load cases D and G, as shown in Fig. 4.5-4 are selected to be critical:

(1) Under load case D, the stringer is subjected to the maximum moment in the negative moment envelope at the left interior support. The unbraced length is equal to half of the stringer span length.

(2) Under load case G, the moment diagram in the left half of the interior span has the most unfavorable shape for Cb factor and the stringer has the least moment resistance.

The moment diagrams for these two critical load cases are given in Fig. 4.5-5.

4.5.3 Additional Bracing

Under the existing bracing plan, the negative moment resistance of the stringer is controlled by lateral torsional buckling in the interior span. As the dimensions (and weight) of the rolled shape are decreased to a certain point, *elastic lateral torsional buckling* becomes the controlling behavior and increased steel yield strength does not help to increase the negative moment resistance. Therefore, at a certain yield strength level, the stringer design will be controlled by elastic lateral torsional buckling under negative bending and the use of higher yield strength will not allow lighter rolled shapes to be used. For this study, as the steel grade increases from 36 ksi (248 Mpa) to 70 ksi (483 Mpa), the minimum weight stringer cross-section decreases from W33X118 to W27X94. However, for higher strength steel, the stringer design is controlled by elastic lateral torsional buckling and cross-section lighter than W27x94 can not be used. Stringer designs under the existing bracing plan are presented in Table 4.5-3.

From the above discussion, it follows that, in order to increase the negative moment capacity in the interior span under negative bending, a shorter unbraced length is necessary. Additional diaphragms were considered for the interior span at a location of 10 ft (3.05 m) from the interior supports. With this additional bracing, the negative bending design is still controlled by lateral torsional buckling in the interior span, but the negative moment resistance is considerably increased, and lighter stringer cross-sections can be used. Stringer designs with the added bracing are presented in Table 4.5-4.

4.5.4 Fatigue Design

The LRFD fatigue code requires that the fatigue design stress range be kept below the nominal fatigue resistance to achieve the desired design life of 75 years. The fatigue design stress range is calculated from the fatigue design moment range, which is the algebraic difference between the positive fatigue moment envelope and the negative fatigue moment envelope. Fatigue moment envelopes for the stringer are shown in Fig. 4.5-6 (live load only) and Fig. 4.5-7 (live load and dead load).

The nominal fatigue resistance depends on the details included in the stringer design. Transverse connection plates are welded to the web at midspan to facilitate the attachment of diaphragms. The connection plates are tight fit to the top flange but kept a certain distance away from the bottom flange (Fig. 4.2-2). In earlier versions of the AASHTO specification, this type of connection plate-to-web detail is a Category C detail. In the AASHTO LRFD specification, it is a Category C' detail, which has a slightly higher fatigue resistance than a Category C detail. Fatigue resistance of the Category C' detail controls the fatigue design of the stringer (Table 4.5-4). A Category A detail, the rolled shape base metal, is also present, but does not control the fatigue design.

For the redesign with the additional diaphragm in the interior span, fatigue is the major concern for high-strength HPS. In order to increase the fatigue resistance, a bolted connection plate-to-web detail with a fatigue Category B designation is considered. Results are presented in Table 4.5-5. As a final step in the stringer redesign study, stringers were also designed for Category A detail at the midspan where the connection

plate-to-web detail is located assuming that this type of detail is available. This connection design would reduce the fatigue problem at the diaphragm locations and would fully reveal the potential for HPS in the stringers. Table 4.5-6 presents the results.

4.5.5 Summary

Table 4.5-7 summarizes the four stringer redesigns developed in this study:

(1) Stringers designed with the existing bracing and the existing welded diaphragm-stringer connection (Category C') detail.

(2) Stringers designed with additional bracing and the existing welded diaphragm-stringer connection (Category C') detail.

(3) Stringers designed with additional bracing and the bolted diaphragm-stringer connection with improved fatigue resistance of a Category B detail.

(4) Stringers designed with additional bracing and an assumed diaphragm-stringer connection with fatigue resistance of a Category A detail.

The information in Table 4.5-7, is plotted in Fig. 4.5-8 to show the relationship between the stringer weight (normalized by the weight of the 50 ksi, or 345 Mpa, design) and steel yield strength under different design conditions.

4.6 Conclusions and Discussion

4.6.1 LFD Versus LRFD

Since the same stringer spacing is maintained in the redesign as that in the original design, the redesign of stringers is comparable with the original design despite the change

in traffic pattern from combined highway and transit traffic to highway traffic only. The design results show that the existing W33X118 A36 design, which used the LFD approach under the earlier version of the AASHTO code, would also satisfy the LRFD code and is the most economic rolled shape for grade 36 ksi (248 Mpa) steel.

4.6.2 Controlling Limit States

The following limit states control the stringer redesigns:

(1) Table 4.5-3 shows that with the existing bracing plan, the *service* limit state controls the stringer design for 36 ksi (248 Mpa) and 50 ksi (345 Mpa) steel; while for 70 ksi (483 Mpa) and 85 ksi (586 Mpa) steel, the stringer design is controlled by *elastic lateral torsional buckling* under negative flexure in the *strength* limit state.

(2) Table 4.5-4 shows that, with additional bracing in the interior span and the welded diaphragm-stringer (Category C') detail, the *service* limit state controls for 36 ksi (248 Mpa) and 50 ksi (345 Mpa) steel, while for 70 ksi (483 Mpa) and 85 ksi (586 Mpa) steel, elastic lateral torsional buckling for the strength limit state does not control, but *fatigue* does control the design.

(3) Table 4.5-5 shows that with additional bracing and the bolted diaphragm-stringer connection detail, the results are the same as in case (2) above. The Category B detail does not appear to alleviate the fatigue problem for 70 ksi (483 Mpa) and 85 ksi (586 Mpa) steel for this particular stringer design, principally because the rolled shapes are available in only discrete sizes.

(4) Table 4.5-6 shows that with the Category A diaphragm-stringer connection detail, *fatigue* does not control the design. For steels with yield strength from 36 ksi (248 Mpa) to 70 ksi (483 Mpa), the *service* limit state controls; while for 85 ksi (586 Mpa) steel, positive bending under the *strength* limit state controls. LRFD allows compact section criteria to be applied to steels with yield strength not exceeding 70 ksi (483 Mpa). Therefore, although a cross-section may satisfy the requirements for compact sections, only the non-compact section moment resistance can be utilized. From Table 4.5-6 it can seen that positive bending controls the stringer design at the 85 ksi (586 Mpa) yield strength level.

In summary, at the lower 36 ksi (248 Mpa) and 50 ksi (345 Mpa) yield strength levels, the *service* limit state controls the stringer design and prevent the use of lighter shapes; while at the higher 70 ksi (483 Mpa) and 85 ksi (586 Mpa) yield strength levels, with additional bracing, *fatigue* is the primary concern.

4.6.3 Potential for HPS in Stringers

Fig 4.5-8 shows that, from 36 ksi (248 Mpa) up to 70 ksi (483 Mpa), weight reduction with increasing yield strength in stringer design is possible, however, for 70 ksi (483 Mpa) and 85 ksi (586 Mpa), *negative bending elastic lateral torsional buckling* or *fatigue* prevents further weight reduction. With adequate bracing to prevent elastic lateral torsional buckling, *fatigue* becomes the controlling factor. Fatigue resistance details for the diaphragm-stringer connection are needed to make use of high strength (yield strength of 85 ksi (586 Mpa) or more) steel. A bolted connection does not appear to provide

sufficiently high fatigue resistance to overcome this problem.

Chapter 5 Potential for High-Performance Steel in Floor Beams

5.1 Introduction

Floor beams are transverse members that carry load from the stringers to trusses at the truss panel points. This chapter investigates the potential for HPS in the floor beams of the Greater New Orleans Bridge #2.

Because of their large dimensions, the floor beams are welded I-shaped girders fabricated from steel plate material. Compared with rolled shapes, steel plate provides a wider range of selection in yield strength. In this study, 50 ksi (345 Mpa), 60 ksi (414 Mpa), 65 ksi (448 Mpa), 70 ksi (483 Mpa), 85 ksi (586 Mpa), 100 ksi (690 Mpa) and 120 ksi (827 Mpa) yield strengths are considered.

5.2 Existing Floor Beam Design

The existing floor beam design for the Greater New Orleans Bridge #2 is shown in Fig. 5.2-1. Top and bottom flanges have the same width which is constant along the floor beam. The center portion of the floor beam has a larger flange thickness than the two side portions. Web height varies along the floor beam and a profile grade of 2.5% is followed. At the profile grade line, which lies under the division between highway and transit traffic on the bridge, the floor beam has the deepest cross section. A longitudinal stiffener is welded on one side of the web at two-fifths of the web height from the top flange, and transverse stiffeners are welded on the other side at the stringer locations. Transverse stiffeners are welded to the top flange and fit tight against the bottom flange.

5.3 General Configuration of Floor Beams in Redesign

Because the redesign considers highway traffic only, floor beams are symmetrical about the bridge transverse centerline. The profile grade line is moved to the center of the floor beam, and the profile grade of 2.5% in the existing design is maintained. Top and bottom flange plates have the same width which is constant along the floor beam. Thickness transitions of flange plates are designed to be located at 22.16 ft (6.75 m) away from the ends of floor beams. Stiffeners are located as in the original design: longitudinal stiffeners on one side at two-fifths the height, and transverse stiffeners on the other side under the stringers. The general configuration of floor beams is shown in Fig. 5.3-1. Although floor beams at different support points under the continuous stringers are subjected to different maximum force effects, in order to simplify fabrication and erection, all floor beams in the suspended span are designed with the same dimensions. Hence, the floor beam design is controlled by the floor beam which is subjected to the largest force effect.

5.4 Analysis of Floor Beams

5.4.1 Analysis Model

Fig. 5.4-1 (a) shows the load transfer among stringers, floor beams, and trusses in the transverse direction. To simplify the analysis, bending moments at the two ends of floor beams are neglected, which leads to the simply supported floor beam analysis model shown in Fig. 5.4-1 (b). Fig. 5.4-1 (b) also indicates the cross sections considered in floor beam design. Each of these cross sections is located under a stringer.

5.4.2 Design Load

The Greater New Orleans Bridge #2 has a total of seven design lanes, as determined by dividing the curb-to-curb distance of 94 ft (28.65 m) by the single lane width of 12 ft (3.66 m). The number of loaded lanes and their positions on the deck must be studied to determine the largest force effect for each cross-section of the floor beam. For each selected number of loaded lanes, the corresponding multiple presence factor (see Table 2.3-1) should be applied. Since the same multiple presence factor (MPF) applies to all cases with more than three lanes loaded, the following cases are considered for the *strength* limit state and *service* limit state:

(1) one lane loaded with a MPF of 1.20;

(2) two lanes loaded with a MPF of 1.00;

(3) three lanes loaded with a MPF of 0.85;

(4) seven lanes loaded with a MPF of 0.65.

For the *fatigue* limit state, only one lane loaded by the design fatigue truck is considered, however, the multiple presence factor of 1.20 for the one lane loaded case is not included for fatigue design according to the LRFD specification.

5.4.3 Load Distribution

The distribution of loads along floor beams and between floor beams in this study is developed using a two part procedure under the assumption that the decking is simply supported between adjacent stringers and the floor beams are nondeflecting:

(1) The deck dead load and design live loads, are first distributed in the *transverse*

direction between stringers assuming the deck is simply supported by the stringers.

(2) The load distributed to each stringer, together with the self weight of the stringer, is then distributed to the floor beams in the *longitudinal* direction by assuming the stringer is a continuous beam resting on nondeflecting floor beams. In this particular bridge, the stringers are either three span continuous or four span continuous.

This simplified procedure for analyzing load effects for floor beams avoids a complicated grillage analysis method but provides reasonable accuracy for the purposes of this study.

The procedure is easily implemented for dead load, however, for live load, a modified procedure was adopted to make it convenient to consider the transverse positioning of the live loads for the maximum force effect:

(i) Different *longitudinal* positions along the stringers are considered separately for the lane load, and truck and tandem loads, to produce the maximum stringer reactions on the floor beam, which are equal to the forces transferred to the floor beams from the stringers.

(ii) The maximum stringer reactions for each type of load are treated as a total load for one lane that is distributed transversely according to the type of load: design lane load is treated as a uniform load; and design truck and design tandem loads are treated as two point loads. Then different numbers of lanes loaded with these converted live loads are considered at different *transverse* positions and distributed among stringers assuming the deck is simply supported to determine stringer reactions that produce the maximum force effect for a particular floor beam cross

section.

For strength limit state and service limit state, Fig. 5.4-2 and Fig. 5.4-3 illustrate the *longitudinal* positions of design lane load, and design truck considered in step (i). The maximum stringer reaction produced by one lane of design lane load is 38.54 kip (171.43 KN). Since the lane load occupies a width of 10 ft (3.05 m), the distributed load considered for distribution in the transverse direction is 3.854 klf (56.25 KN/m). The maximum stringer reaction due to the design tandem is less than that due to the design truck, therefore, only the design truck is considered for transverse distribution. The maximum reaction produced by the design truck is 68.21 kip (303.41 KN), therefore the point loads considered for transverse distribution are 34.105 kip (151.71 KN) at 6 ft (1.83 m) apart. The truck positions considered for fatigue limit state are the same as those shown in Fig. 5.4-3, except that the main axle spacing is 30 ft (9.14 m) instead of 14 ft (4.27 m).

For each floor beam cross section indicated in Fig. 5.4-1, the four cases listed in Section 5.4.2 with the most critical *transverse* positioning of live loads within each lane are considered for the strength limit state and the service limit state. Fig. 5.4-4 shows the critical positions of lanes and live loads within each lane for floor beam cross section No. 6. The positions for cross section No. 7 are illustrated in Fig. 5.4-5. Fatigue only needs to consider the one fatigue truck case, which has a critical position similar to that of one-lane loaded case under the strength limit state.

5.5 Redesign of Floor Beams

5.5.1 General

The floor beams are designed as non-composite members. For shear requirement under the strength limit state, only the shear force at the end section of the floor beam needs to be considered, since the cross sectional area of the floor beam is at its minimum value and the shear force is at its maximum value. Bending moments at the cross sections indicated in Fig. 5.4-1 (b) were calculated for the strength, service, and fatigue limit states to provide the floor beam design moment envelopes. The results of these calculations show that the seven-lane loaded case controls the floor beam design bending moment and shear for the strength and service limit states.

5.5.2 Design Tool

A floor beam optimization program was developed for floor beam redesign. Floor beam designs with the minimum total weight are considered to be optimum. The optimization program uses a brute force iteration strategy to search for optimum floor beam dimensions. The following dimensions were considered: (1) web thickness, (2) web height at the center line (profile grade line), (3) flange width, (4) flange thickness in the center portion, and (5) flange thickness in the side portions. Ranges and increments for these five iteration variables are specified by the user.

During the iteration process, the stringer-deck dead load effects and the maximum live load effects are constant. Dead load effects due to the self weight of the floor beam are calculated during execution of the program for each particular floor beam design.

The optimization program checks the *bending moment* requirement for the strength limit state, the service limit state, and the fatigue limit state at: (1) the center cross section, and (2) the flange plate thickness transition cross section. For the *shear* requirement, the end section is checked.

5.5.3 Fatigue Design

For fatigue design, only the bottom flange region needs to be checked since the top flange region is never in tension. Transverse stiffeners welded to the web control the fatigue design of the floor beams. These are category C' details in the LRFD specification. Two Category B details are present in the floor beam, but do not control fatigue design: (1) the flange plate thickness transition, (2) the continuous flange-web fillet weld.

5.5.4 Impact of Stringer Design on Floor Beam Design

Chapter 4 discusses stringer designs for different steel yield strengths. The impact of the stringer design on floor beam design was studied. Calculations show that different stringer designs create negligible differences in the floor beam design moment and shear. Therefore, throughout the redesign of floor beams, only the existing stringer design, W33X118 of A36 steel, is considered.

5.5.5 Optimum Floor Beam Designs

Minimum weight floor beam designs were generated by the optimization program

for steel yield strength levels of 50 ksi (345 Mpa), 60 ksi (414 Mpa), 65 ksi (448 Mpa), 70 ksi (483 Mpa), 85 ksi (586 Mpa) and 100 ksi (690 Mpa). In this study, the increment for web and flange plate thicknesses is 1/8 in (3.18 mm). For web height, it is 1 in (25.40 mm). Optimum floor beam designs are given in Table 5.5-1.

Fig. 5.5-1 shows the weight of the minimum weight designs versus the steel yield strength. As the steel yield strength is increased, the floor beam weight is reduced.

Fig 5.5-2 shows the web thickness of the minimum weight designs versus the steel yield strength. The figure shows that the web thickness does not change continuously with steel yield strength, because the plate thickness increment was 1/8 in (3.18 mm).

Fig. 5.5-3 shows the web height of the minimum weight designs versus the steel yield strength. Web height decreases with increasing steel yield strength, except that at the point where the web thickness changes.

5.5.6 Floor Beams with Constant Depth

The LRFD code specifies that compact section design criteria can be used only for constant depth sections with yield strength not exceeding 70 ksi (483 Mpa). Floor beams in the Greater New Orleans Bridge #2 have variable depth, which requires that the floor beams be designed using non-compact criteria. To study the impact of using the full plastic moment capacity of the floor beam according to compact section design criteria, floor beams with constant depth and the same flange thickness transition locations were designed. Results are given in Table 5.5-2.

5.6 Conclusions and Discussion

5.6.1 Controlling Limit States

Table 5.5-1 shows that the *strength* and *service* limit states control the floor beam design in the Greater New Orleans Bridge #2. The *fatigue* limit state has a fairly large safety margin even for steel with 120 ksi (827 Mpa) yield strength, although it appears that at higher yield strength levels, fatigue will control eventually.

5.6.2 Constant Depth Versus Variable Depth Floor Beams

A comparison between Table 5.5-1 and Table 5.5-2 shows that, although the constant depth design allows compact section design criteria to be used, the variable depth section designs give the minimum weight design for all strength levels considered. It follows that, the 70 ksi (483 Mpa) limitation on the use of compact section criteria is not an obstacle to the use of high-strength HPS for floor beams in the Greater New Orleans Bridge #2.

5.6.3 Potential for High-Performance Steel in Floor Beams

It can be concluded that for the Greater New Orleans Bridge #2, the increased strength of HPS can be fully utilized.

Chapter 6 Potential for High-Performance Steel in Truss Members

6.1 Introduction

This chapter discusses the potential for high-performance steel in truss member design. Truss members in the Greater New Orleans Bridge #2 are comprised of box shape members fabricated from steel plates through welding or bolting. In this study, HPS with yield strengths of 50 ksi (345 Mpa), 60 ksi (414 Mpa), 65 ksi (448 Mpa), 70 ksi (483 Mpa), 85 ksi (586 Mpa), 100 ksi (690 Mpa) and 120 ksi (827 Mpa) are investigated for truss members in the suspended span.

Connection design often determines the usable strength of a truss member. Since the objective of this study is to investigate the potential for high-performance steel used in truss members as base metal, it is assumed that the connections can be designed so that they have no influence on the load capacity of the truss members. Under this assumption, the design of tension members is quite simple and the relationship between material cost and strength is apparent: the gross area of a tension member will decrease in proportion to the increasing yield strength of steel (neglecting the slenderness criteria for tension members). Therefore, this study focused on the compression members of the Greater New Orleans Bridge #2.

6.2 Existing Truss Design

Truss members in the existing Greater New Orleans Bridge #2 are of two types of built-up box shapes, as shown in Fig. 6.2-1. Type I members, which are usually

compression members, are welded boxes with one perforation at each end. Type II members, which are usually tension members, are bolted boxes with perforations along the full length. Truss members are connected through bolted connection at the truss panel points. This requires that the member width, which is the distance between the outside surfaces of the web plates of the truss members, is constant along the whole bridge. In the existing design of this bridge, the member width is 36 in (914.4 mm). The truss member types in the redesign are the same as those in the existing design.

6.3 Analysis of Trusses

There are two parallel trusses in the Greater New Orleans Bridge #2. Each truss is analyzed as a planar truss with loads applied at the panel points. Truss members are analyzed as pin-ended for axial force calculation. The design loads for the floor beam design (Section 5.4.2) also apply to the truss design. In addition to axial forces, dead load moment due to the self-weight of a truss member is taken into consideration.

Two assumptions are used in distributing the loads acting on the floor system to the trusses:

(1) The deck and the stringers are assumed to be simply supported between adjacent floor beams.

(2) The floor beams are assumed to be simply supported at truss panel points.

With these assumptions, the distribution of loads from the deck to the trusses is a three-step process: (1) loads acting on the deck are longitudinally distributed to floor beams through the simply supported deck and stringer; (2) the loads acting on floor

beams are distributed transversely between the two trusses by treating the floor beams as simply supported on the truss panel points; and (3) load distribution among the members of a truss due to the concentrated loads acting on the panel points are found through structural analysis of the truss. The dead loads of the laterals and portal frames are divided equally between the two trusses.

Based on the load distribution process described above, an axial force influence line can be calculated for each truss member to address steps (1) the longitudinal distribution of loads and (3) load distribution within a truss. Fig. 6.3-1 shows the influence lines for some truss members in the suspended span. As noted earlier, the suspended span is simply supported on the cantilever spans and can be analyzed separately.

A procedure to calculate an equivalent number of design lanes for one truss is illustrated in Fig. 6.3-2. The purpose of the procedure is to determine the largest force effect in the truss members for the *strength* limit state and the *service* limit state, considering the transverse position of the live loads, the number of lanes loaded, and the multiple presence factors. The procedure corresponds to step (2) of the load distribution process discussed above. To determine the largest force effects under strength and service limit states, one-lane loaded, two-lane loaded, three-lane loaded and seven-lane loaded cases are considered with the proper multiple presence factors. A unit patch load is applied in each lane and the reaction at the center line of the truss is calculated and then multiplied by the multiple presence factor to determine an equivalent number of design lanes for the truss. Lanes and loads are positioned as close as possible to the truss being

considered to produce largest reaction at the center line of the truss. For the strength and service limit states, the seven-lane loaded case gives the largest equivalent number of design lanes (i.e., produces the largest force effect for the truss). For the *fatigue* limit state, the transverse positioning is the same as that of one-lane loaded case for *strength* limit state except that the one-lane loaded multiple presence factor of 1.20 is not used. It should be noted that, the equivalent number of design lanes is different from the number of design lanes for the whole bridge and is used for truss member design only.

In summary, the design axial force for a truss member is calculated through the following steps:

(1) Determine the axial force influence line for the truss member.

(2) Find the maximum axial force in the truss member by positioning one lane of design loads longitudinally along the influence line. For the strength limit state and the service limit state, the design loads include the combination of design lane load and design truck, and the combination of design lane load and design tandem. For fatigue, only one lane with the design fatigue truck is considered.

(3) Multiply the maximum axial force with the equivalent number of design lanes for the truss to get the actual design force for the truss member.

Table 6.3-1 gives the design axial forces for members in the suspended span under the strength limit state of the LRFD code.

6.4 Redesign of Compression Members

6.4.1 Introduction

To find the box shape with the minimum weight cross section, a compression member optimization program was developed. The compression member optimization program uses brute force iteration to search for the optimum component plate dimensions for a compression member under the design conditions set by the user, which include limitations on the width and height of the box member, and the yield strength of steel. The design axial force and the bending moment due to self weight of the member are taken into consideration.

The optimization program considers the *strength* limit state and the *fatigue* limit state for a compression member. The *service* limit state is neglected. For the fatigue limit state, the continuous web-cover plate fillet weld in the compression members is a category B detail which controls the fatigue design.

6.4.2 Redesign of Top Chord SU5-SU7

SU5-SU7 is a top chord near the center line of the bridge. It has the largest design axial compression force in the suspended span. Using the compression member optimization program, minimum weight designs for different steel yield strength levels are generated for member SU5-SU7 under different values of the member width constraint. The width constraint was imposed because of the need to connect the members together. Fig 6.4-1 shows the gross area of the minimum weight design versus the member width for several of the yield strength levels considered. The safety margins of

these designs are shown in Fig 6.4-2, and the thicknesses of the cover plates are shown in Fig 6.4-3.

For each yield strength level, the minimum gross area remains almost constant over a certain range of member widths. Within this range, overall buckling of the truss member controls its design, safety margins are at a minimum level, and the strength of the steel is fully utilized. Above this range, the minimum weight gross area increases in a nearly linear fashion with the member width, because as the member width increases, thicker cover plates (Fig. 6.4-3) are needed to prevent local buckling. As a result, the member strength becomes excessive and a large safety margin exists. Truss members in this member width region are not economical.

If the minimum weight gross area versus member width curves for different steel yield strengths are considered together, the curves can be divided into three regions depending on member width, as indicated in Fig. 6.4-1: (1) region A covers small member widths, for which the gross area of the member decreases with increasing yield strength, and higher strength steels provide reduced weight compared with lower strength steels; (2) region B covers intermediate member widths, for which the gross area decreases with increasing yield strength to a certain point, then increases, and thus an optimum yield strength exists which gives the minimum weight design; (3) region C covers large member widths, for which the gross area increases with increasing yield strength and the use of high-strength steels are not justified. The different relationships between the minimum weight gross area and the steel yield strength for these three regions are presented in Fig. 6.4-4 for top chord SU5-SU7.

Fig. 6.4-5 shows the safety margins for member SU5-SU7 under the *fatigue* limit state. The figure shows that the factored live load stress range is less than 10% of the nominal fatigue resistance for all cases considered. Thus, fatigue does not control the design at any yield strength level.

6.4.3 Comparison of Redesigns of Members SU1-SU3, SU3-SU5 and SU5-SU7

SU1-SU3 and SU3-SU5 are two other top chord members in the suspended span, and SU1-SU3 is subjected to the smallest design compression force in that span. Fig. 6.4-6 and Fig. 6.4-7 give their minimum weight gross area versus member width curves.

The curves of these two members have the same features as those of member SU5-SU7 discussed above. However, by referring to Table 6.3-1 for the design axial forces of these three members, and comparing Fig. 6.4-7, Fig. 6.4-6 and Fig. 6.4-1, it can be seen that as the design axial force increases, regions A and B grow to include larger member widths. This suggests that higher strength steels can be economically used in a wider range of member widths for compression members loaded with higher axial force.

To study the impact of the design axial force on the weight reduction possible from using HPS, the minimum weight gross area (normalized by the minimum weight gross area using 50 ksi (345 Mpa) yield strength steel) was plotted versus the steel yield strength. The plots are shown for members SU1-SU3, SU3-SU5 and SU5-SU7 in Fig. 6.4-8 (a), (b) and (c) for member width constrained to three different values: 28 in (711.2 mm), 32 in (812.8 mm) and 36 in (914.4 mm). All of these member widths are in region A (for which increased steel yield strength provides reduced member gross area) for the

three members except that the 32 in (812.8 mm) and 36 in (914.4 mm) member width are in region B for member SU1-SU3. Fig. 6.4-8 shows that SU5-SU7, which has the largest design compression force, has the largest reduction in weight with increased yield strength, and SU1-SU3, which has the smallest design axial force, has the smallest reduction in weight with increased yield strength. Comparison of Fig. 6.4-8 (a), (b) and (c) shows that the possible weight savings depends on member width.

6.5 Conclusions and Discussion

6.5.1 Controlling Limit States

For the truss members that were studied, *strength* was the controlling limit state and *fatigue* was not a concern.

6.5.2 Potential for HPS in Compression Truss Members

From the redesigns described earlier, it can be concluded that efficient use of HPS in compression truss members is related to (1) the member width, and (2) the design axial force. Depending on the design axial force of a truss member, the member width can be divided into three regions where HPS shows different potential: (1) for smaller member widths (region A), steel yield strength reduces member weight and HPS can be used efficiently; (2) for intermediate member widths (region B), an optimum steel yield strength exists which gives the minimum member weight; (3) for larger member widths (region C), increases in yield strength increase member weight and the use of HPS is not beneficial. For smaller member widths (region A), greater weight savings can be achieved

using HPS for compression members with larger design axial forces. Thus, HPS can be used most efficiently in highly loaded compression members with small member widths.

Chapter 7 Limitations and Recommendations

7.1 Summary of Conclusions

The potential for high-performance steel in stringers, floor beams, and truss members of the Greater New Orleans Bridge #2 can be summarized as follows:

(1) With current bridge configurations and design code requirements, HPS with yield strength from 36 ksi (248 Mpa) to 70 ksi (483 Mpa) can be used economically in stringers designed as rolled shapes. Above 70 ksi (483 Mpa), fatigue prevents further weight reduction with increasing yield strength. Fatigue resistant details for the diaphragm-stringer connections are needed to make efficient use of steels with yield strength higher than 70 ksi (483 Mpa).

(2) In floor beams which are designed as welded I-shaped girders, the potential for HPS can be fully utilized, resulting in weight reduction with increasing yield strength for the range of steel yield strengths considered.

(3) In tension truss members, member weight decreases in proportion with increasing steel yield strength, however, in compression truss members, the decrease in weight that can be achieved depends on the axial force level, and the decrease in weight with increasing yield strength is larger for members with larger axial forces.

7.2 Limitations of Study

The results of this study are limited by the following conditions:

(1) The redesign of the stringers, floor beams, and truss members using HPS are primarily based on the existing configuration of the Greater New Orleans Bridge #2. The redesigns were optimized at the member level. However, at the system level, these designs might not be optimum.

(2) The relative cost of the various strength levels of HPS were not considered. The cost of HPS is likely to increase with yield strength. Since the composition and/or processing practices for HPS are likely to differ from those of currently-available high-strength steel, the cost factors for currently-available high-strength steel may not apply.

(3) Only the weight savings from using HPS were evaluated. The benefits of the improved weldability, fracture toughness, corrosion resistance, and other properties of HPS were not considered.

(4) The costs of fabrication, erection, and maintenance were not considered.

(5) Structural analysis was simplified to allow design parameters to be varied easily.

(6) Construction strength and stability for stringers, floor beams, and truss members were not considered.

(7) The minimum weight members that were designed may be difficult to handle and erect.

(8) Connections for truss members were not considered in detail. A width constraint on the truss members, to facilitate connection between members, was considered.

(9) Stringers were designed as non-composite girders. The Category B bolted stringer-diaphragm connection detail may show some advantages over the Category C' welded detail if the stringers were designed as composite girders.

7.3 Recommendations for Further Study

Due to the limitations of this study, further work is needed to fully investigate the potential for high-performance steel in the Greater New Orleans Bridge #2:

(1) Design the stringers as composite girders and investigate the potential for HPS.

(2) Use life cycle engineering concepts to evaluate the impact of HPS on the cost of material, fabrication, erection, and maintenance of the bridge. Using this approach, properties of HPS other than strength, such as improved weldability, fracture toughness, and corrosion resistance, can be considered.

(3) When HPS is commercially produced, reevaluate the potential for HPS in bridge designs using the relative costs of different yield strength levels.

In addition, the potential for HPS in bridges with configurations and member cross-sectional shapes that are different from those of the Greater New Orleans Bridge #2 should also be investigated. Further research is needed to develop fatigue resistant details for stringer-diaphragm connections.

References

1. **AASHTO (1989)** *Standard Specification for Highway Bridges, Fourteenth Edition*, American Association of State Highway and Transportation Officials, Washington D.C.

2. **AASHTO (1993)** *Load and Resistance Factor Design Specification for Highway Bridges*, American Association of State Highway and Transportation Officials, Washington D.C.

3. **Graville (1976)** *Cold Cracking in Welds in HSLA Steels, Proceedings of HSLA Micro Alloyed Structural Steels*, American Society for Metals, Metals Park, Ohio

Table 2.1-1 Values of η_D, η_R and η_I

Limit State	η_D		η_R		η_I	
	Non-ductile	Ductile	Non-redundant	Redundant	with operational importance	otherwise
Strength	1.05	0.95	1.05	0.95	≥ 1.05	≥ 0.95
Service	1.0		1.0		N/A	
Fatigue	1.0		1.0		N/A	
Extreme Event	1.0		1.0		≥ 1.05	≥ 0.95

Table 2.2-1 LRFD Load Factors (a partial list)

Load Combinations	Dead Load				Live Load
	DC		DW		LL
Strength I	Maximum	1.25	Maximum	1.50	1.75
	Minimum	0.90	Minimum	0.85	
Service II	1.00		1.00		1.30
Fatigue	N/A		N/A		0.75

DC: Components and Attachments DW: Wearing Surface and Utilities
LL: Vehicular Live Loads

Table 2.3-1 Multiple Presence Factors

Number of Loaded Lanes	Multiple Presence Factors
1	1.20
2	1.00
3	0.85
>3	0.65

Table 2.3-2 Impact Factors

Component	Impact Factors (IM)
Deck Joints - All Limit States	75%
All Other Components • Fatigue and Fracture Limit State	15%
• All Other Limit States	33%

Table 2.4-1 Live Load Distribution Factors for Stringers

Moment	Interior Stringers	One Lane Loaded	$0.5\left[0.12+\left(\frac{S}{2.5}\right)^{0.4}\left(\frac{S}{L}\right)^{0.3}\left(\frac{K_g}{12.0Lt_s^3}\right)^{0.1}\right]$
		Two or More Lanes Loaded	$0.5\left[0.15+\left(\frac{S}{3.0}\right)^{0.6}\left(\frac{S}{L}\right)^{0.2}\left(\frac{K_g}{12.0Lt_s^3}\right)^{0.1}\right]$
	Exterior Stringers	One Lane Loaded	Lever Rule
		Two or More Lanes Loaded	$g = e\, g_{interior}$ $e=\frac{7+d_e}{9.1}\geq 1.0$
Shear	Interior Stringers	One Lane Loaded	$0.36+\frac{S}{25.0}$
		Two or More Lanes Loaded	$0.5\left[0.4+\frac{S}{6}-\left(\frac{S}{25}\right)^{2.0}\right]$
	Exterior Stringers	One Lane Loaded	Lever Rule
		Two or More Lanes Loaded	$g = e\, g_{interior}$ $e=\frac{6+d_e}{10}$

g = distribution factor
S= spacing of stringers
L = span of stringers
t_s = depth of concrete deck
e = correction factor
d_e = distance between the center of exterior beam and the interior edge of curb or traffic barrier

$$K_g=n\left(I+Ae_g^2\right)$$

n = modular ratio between steel and concrete
I = inertia of stringer (in^4)
A= area of stringer
e_g= distance between the centers of gravity of stringer and deck

Table 4.5-1 Comparison of Analysis Results for 3 Span and 4 Span Continuous Stringers

No. of Spans	Strength Limit State			Service Limit State	Fatigue Limit State
	Maximum Moment (kip-ft)		Maximum Shear	Maximum Moment	Maximum Moment
	Positive	Negative	(kips)	(kip-ft)	(kip-ft)
3	1149	-956	156	859	145
4	1138	-986	156	850	145

Note: Moments and shears are factored.

Span No. [1]	Node No. [1]	Distance [2]	Lane Load Range	Controlling Concentrated Load [5]				Design Load Case
				Type	Position [4]	Main Axle Spacing (ft)	Direction	
1	2	0.1	[1,2]	Truck	1.12	14	Left	A
1	3	0.2	[1,2]	Truck	1.12	14	Left	A
1	4	0.3	[1,2]	Truck	1.12	14	Left	A
1	5	0.4	[1,2]	Truck	1.12	14	Left	A
1	6	0.5	[1,2]	Truck	1.12	14	Left	A
1	7	0.6	[1,2]	Truck	1.12	14	Left	A
1	8	0.7	[1,2]	Truck	1.12	14	Left	A
1	9	0.8	[0,0.24],[1,2]	Truck	1.12	14	Left	B
1	10	0.9	[0,0.76],[1,2]	Truck	1.12	14	Left	C
Support	11	1.0	[0,2]	Truck	0.88	14	Right	D
2	12	1.1	[0,1],[1.28,2]	Truck	0.88	14	Right	E
2	13	1.2	[0,1]	Truck	0.88	14	Right	F
2	14	1.3	[0,1],[2,3]	Truck	0.88	14	Right	G
2	15	1.4	[0,1],[2,3]	Truck	0.88	14	Right	G
2	16	1.5	[0,1],[2,3]	Truck	0.88	14	Right	G

Note:

[1] Span and node numbers follow the stringer analysis model as shown in Fig. 4.4-2.

[2] Distances are given as the distances to the left support divided by the span length L = 49'2-3/4''.

[3] Lane Load range is given as a pair of distances to the left support divided by the span length.

[4] Truck position is given as the distance from the left support to the front axle divided by the span length.

[5] Concentrated load refers to truck, tandem or two truck load. In this particular bridge, negative moment envelope is controlled by the truck and lane load combination.

Table 4.5-2 Vehicular Live Load Positions for Maximum Negative Moment Under Strength Limit State in Stringer Design

Table 4.5-3 Stringer Designs with Existing Bracing and Category C' Fatigue Details

Steel Yield Strength(ksi)	Shape	Adequate Design	Controlling Limit State	Strength Limit State							Service Limit State	Fatigue Limit State (Category C')
				Bending						Shear		
				Positive		Negative						
						Load Case D		Load Case G				
				Compactness	Safety Margin	Compactness	Safety Margin	Compactness	Safety Margin	Safety Margin	Safety Margin	Safety Margin
36	W33x118	Yes	Service	Compact	7.7%	InE LTB	11.2%	InE LTB	22.1%	56.9%	0.3%	65.3%
50	W30X99	Yes	Service	Compact	14.0%	E LTB	13.2%	E LTB	13.3%	63.7%	6.8%	38.2%
	W27X94	No		Compact	4.9%	E LTB	7.7%	E LTB	7.8%	57.2%	-1.7%	14.4%
70	W27X94	Yes	Strength	Compact	32.0%	E LTB	7.7%	E LTB	7.8%	69.4%	27.4%	14.4%
	W27X84	No	(Neg. Bending)	Non-compact	12.3%	E LTB	-11.7%	E LTB	-11.5%	67.5%	18.1%	1.6%
85	W27X94	Yes	Strength	Non-compact	34.0%	E LTB	7.7%	E LTB	7.8%	74.8%	40.2%	14.4%
	W27X84	No	(Neg. Bending)	Non-compact	27.8%	E LTB	-11.7%	E LTB	-11.5%	73.2%	29.4%	1.6%

Table 4.5-4 Stringer Designs with Additional Bracing and Category C' Fatigue Details

Steel Yield Strength(ksi)	Shape	Adequate Design	Controlling Limit State	Strength Limit State							Service Limit State	Fatigue Limit State (Category C')
				Bending						Shear		
				Positive		Negative						
						Load Case D		Load Case G				
				Compactness	Safety Margin	Compactness	Safety Margin	Compactness	Safety Margin	Safety Margin	Safety Margin	Safety Margin
36	W33x118	Yes	Service	Compact	7.7%	InE LTB	11.2%	InE LTB	22.1%	56.9%	0.3%	65.3%
50	W30X99	Yes	Service	Compact	14.0%	E LTB	13.2%	E LTB	13.3%	63.7%	6.8%	38.2%
	W27X94	No		Compact	4.9%	E LTB	7.7%	E LTB	7.8%	57.2%	-1.7%	14.4%
70	W27X84	Yes	Fatigue	Non-compact	12.3%	InE LTB	26.9%	InE LTB	35.7%	67.5%	14.3%	14.4%
	W24X76	No		Compact	8.5%	InE LTB	13.1%	InE LTB	23.6%	61.8%	2.8%	-47.9%
85	W27X84	Yes	Fatigue	Non-compact	27.8%	InE LTB	40.0%	InE LTB	47.1%	73.2%	32.5%	1.6%
	W24X76	No		Non-compact	14.3%	InE LTB	13.1%	InE LTB	23.6%	68.5%	16.2%	-47.9%

Table 4.5-5 Stringer Designs with Additional Bracing and Category B Fatigue Details

Steel Yield Strength(ksi)	W-Shape	Adequate Design	Controlling Limit State	Strength Limit State							Service Limit State	Fatigue Limit State (Category B)
				Bending						Shear		
				Positive		Negative						
						Load Case D		Load Case G				
				Compactness	Safety Margin	Compactness	Safety Margin	Compactness	Safety Margin	Safety Margin	Safety Margin	Safety Margin
36	W33x118	Yes	Service	Compact	7.7%	InE LTB	11.2%	InE LTB	22.1%	56.9%	0.3%	73.9%
50	W30X99	Yes	Service	Compact	14.0%	E LTB	13.2%	E LTB	13.3%	63.7%	6.8%	53.7%
	W27X94	No		Compact	4.9%	E LTB	7.7%	E LTB	7.8%	57.2%	-1.7%	35.8%
70	W27X84	Yes	Fatigue	Non-compact	12.3%	InE LTB	26.9%	InE LTB	35.7%	67.5%	14.3%	26.2%
	W24X76	No		Compact	8.5%	InE LTB	13.1%	InE LTB	23.6%	61.8%	2.8%	-10.9%
85	W27X84	Yes	Fatigue	Non-compact	27.8%	InE LTB	40.0%	InE LTB	47.1%	73.2%	32.5%	26.2%
	W24X76	No		Non-compact	14.3%	InE LTB	13.1%	InE LTB	23.6%	68.5%	16.2%	-10.9%

Table 4.5-6 Stringer Designs with Additional Bracing and Category A Fatigue Details

Steel Yield Strength(ksi)	Shape	Adequate Design	Controlling Limit State	Strength Limit State							Service Limit State	Fatigue Limit State (Category A)
				Bending						Shear		
				Positive		Negative						
						Load Case D		Load Case G				
				Compactness	Safety Margin	Compactness	Safety Margin	Compactness	Safety Margin	Safety Margin	Safety Margin	Safety Margin
36	W33x118	Yes	Service	Compact	7.7%	InE LTB	11.2%	InE LTB	22.1%	56.9%	0.3%	82.6%
50	W30X99	Yes	Service	Compact	14.0%	E LTB	13.2%	E LTB	13.3%	63.7%	6.8%	69.1%
	W27X94	No		Compact	4.9%	E LTB	7.7%	E LTB	7.8%	57.2%	-1.7%	57.2%
70	W24X76	Yes	Strength	Compact	8.5%	InE LTB	13.1%	InE LTB	23.6%	61.8%	2.8%	26.0%
	W24X68	No		Compact	-2.4%	InE LTB	1.6%	InE LTB	13.5%	59.5%	-10.0%	18.1%
85	W24X68	Yes	Strength	Non-compact	3.1%	InE LTB	19.0%	InE LTB	28.8%	66.7%	9.4%	18.1%

Table 4.5-7 Summary of Stringer Designs

Yield Strength (ksi)	Without Additional Bracing		With Additional Bracing					
	Category C '		Category C '		Category B		Category A	
	Shape	Weight *	Shape	Weight	Shape	Weight	Shape	Weight
36	W33X118	119.2%	W33X118	119.2%	W33X118	119.2%	W33X118	119.2%
50	W30X99	100.0%	W30X99	100.0%	W30X99	100.0%	W30X99	100.0%
70	W27X94	94.9%	W27X84	84.8%	W27X84	84.8%	W24x76	76.8%
85	W27X94	94.9%	W27X84	84.8%	W27X84	84.8%	W24X68	68.7%

Note :

* Stringer weight is normalized with respect to stringer design for steel with a 50 ksi(345 Mpa) yield strength.

Table 5.5-1 Minimum Weight Design of Floor Beams with Variable Depth

Steel Yield Strength (ksi)	Floor Beam Weight (kips)	Floor Beam Dimensions					Safety Margin (%)			
		Web		Flange			Moment			Shear
		Thickness (in)	Depth (in) At Midspan	Thickness (in) At Thickness Transition	Thickness (in) At Midspan	Width (in)	Strength	Service	Fatigue	
50	43.10	0.500	140	1.500	2.500	14	1.1	1.5	64.6	13.8
60	39.67	0.500	130	1.125	1.875	17	3.4	3.8	58.4	8.3
65	37.87	0.500	120	1.375	2.250	14	0.5	0.9	53.6	2.1
70	36.69	0.500	120	1.250	2.125	14	3.6	4.0	51.6	2.1
85	35.40	0.625	120	0.875	1.750	11	0.4	0.9	39.2	49.9
100	32.76	0.625	110	0.875	1.625	11	0.2	0.7	28.2	46.5
120	30.40	0.625	90	1.125	1.875	11	0.7	1.1	14.1	38.6

Table 5.5-2 Minimum Weight Design of Floor Beams with Constant Depth

Steel Yield Strength (ksi)	Floor Beam Weight (kips)	Floor Beam Dimensions					Safety Margin (%)			
		Web		Flange			Moment			Shear
		Thickness (in)	Depth (in) At Midspan	Thickness (in) At Thickness Transition	Thickness (in) At Midspan	Width (in)	Strength	Service	Fatigue	
50	43.19	0.500	140	1.500	2.500	14	1.1	1.5	64.6	20.7
60	39.76	0.500	130	1.125	1.875	17	3.4	3.8	58.4	16.0
65	37.96	0.500	120	1.250	2.125	15	0.8	1.3	54.0	10.6
70	36.78	0.500	120	1.250	2.125	14	3.6	4.0	51.6	10.6
85	33.74	0.500	110	1.375	2.250	12	4.9	5.3	41.8	4.7
100	32.88	0.625	110	0.875	1.625	11	0.2	0.7	28.2	51.3
120	30.51	0.625	90	1.125	1.875	11	0.7	1.1	14.1	44.2

Table 6.3-1 Axial Forces for Truss Members in Suspended Span

Member	Unfactord (kips)		Factored (kips)		
	DL	LL+IM	DL	LL+IM	Total
SU1-SU3	-4137	-782	-5296	-1368	-6980
SU3-SU5	-6914	-1306	-8851	-2286	-11665
SU5-SU7	-8319	-1570	-10650	-2747	-14032
SL0-SL2	2251	422	2882	739	3792
SL2-SL4	5693	1076	7288	1884	9606
SL4-SL6	7788	1470	9970	2573	13137
SL6-SL6'	8496	1602	10877	2803	14328
SL0-SU1	-4557	-855	-5832	-1496	-7676
SU1-SL2	3799	747	4864	1308	6465
SL2-SU3	-3124	-646	-3999	-1130	-5372
SU3-SL4	2440	552	3124	966	4283
SL4-SU5	-1747	-464	-2237	-812	-3194
SU5-SL6	1056	384	1352	672	2120
SL6-SU7	-356	-311	-456	-544	-1047
TYP HANGER	438	285	566	499	1116
SL0-CU9	4551	842	5826	1473	7645

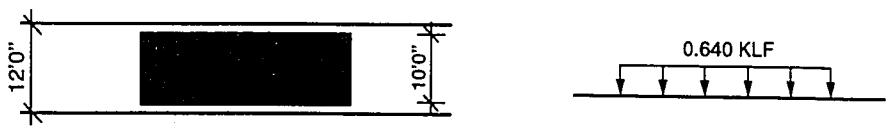

(a) Design Lane Load

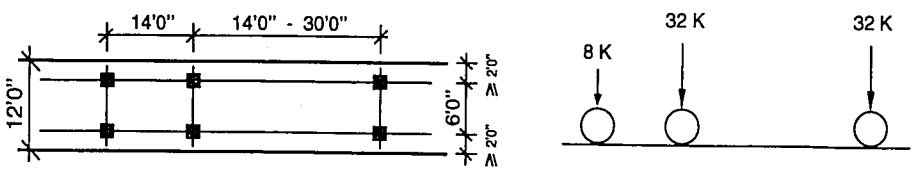

(b) Design Truck

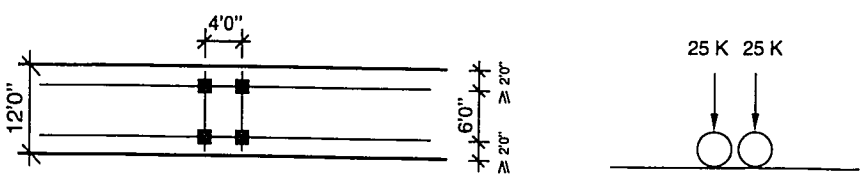

(c) Design Tandem

Fig. 2.3-1 LRFD Vehicular Live Loads

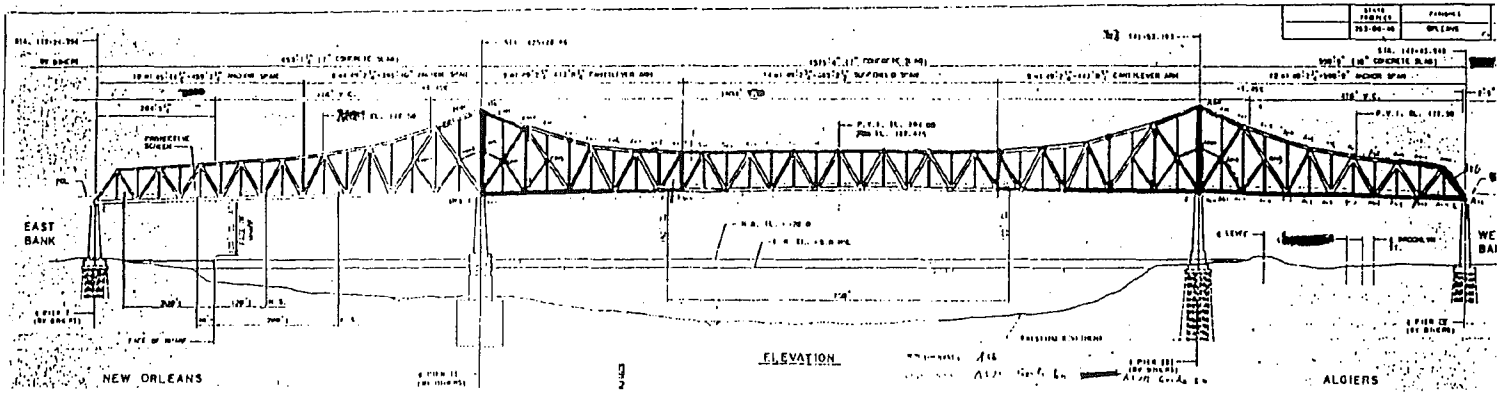

Fig. 3.1-1 Elevation of the Greater New Orleans Bridge #2

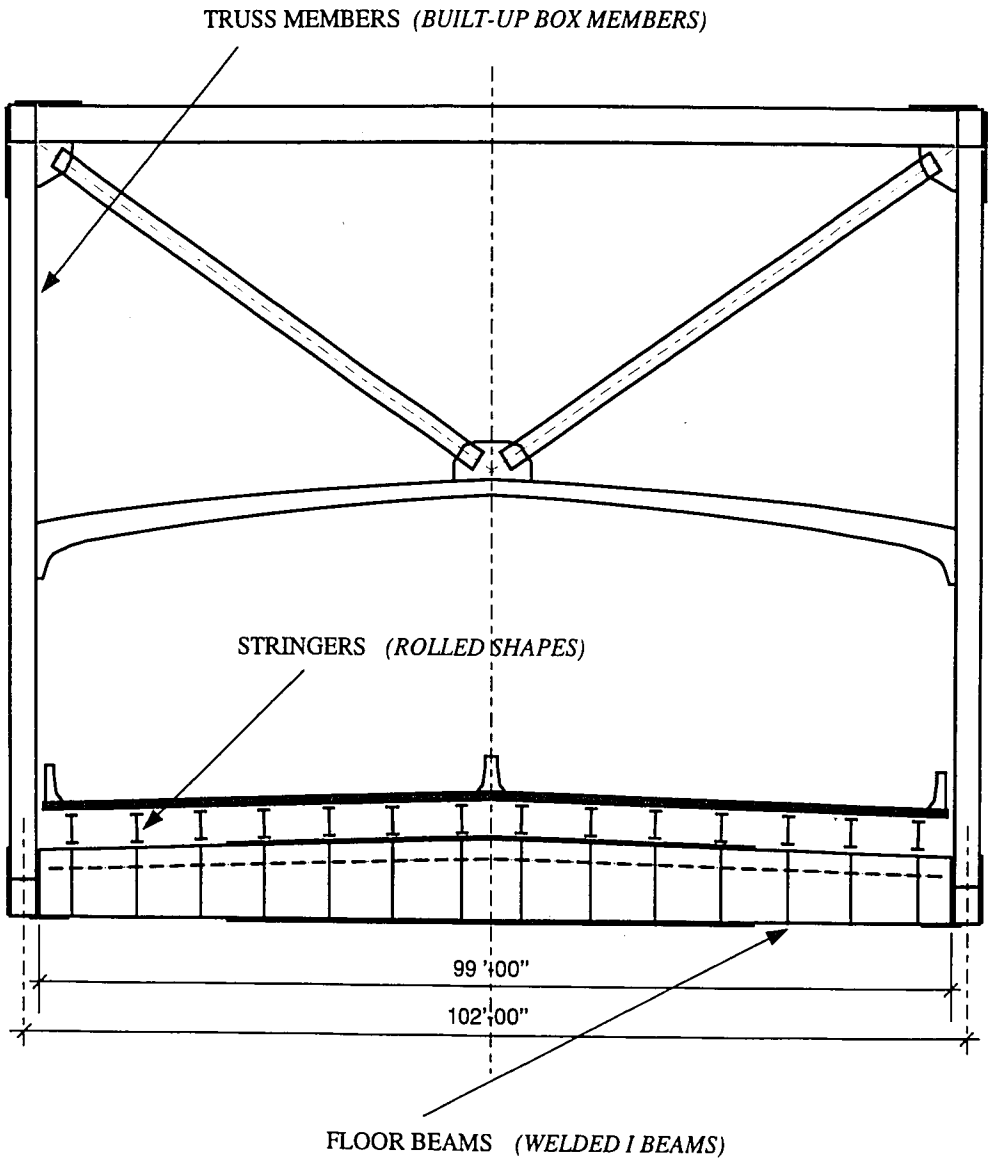

Fig. 3.1-2 Typical Cross Section of Suspended Span

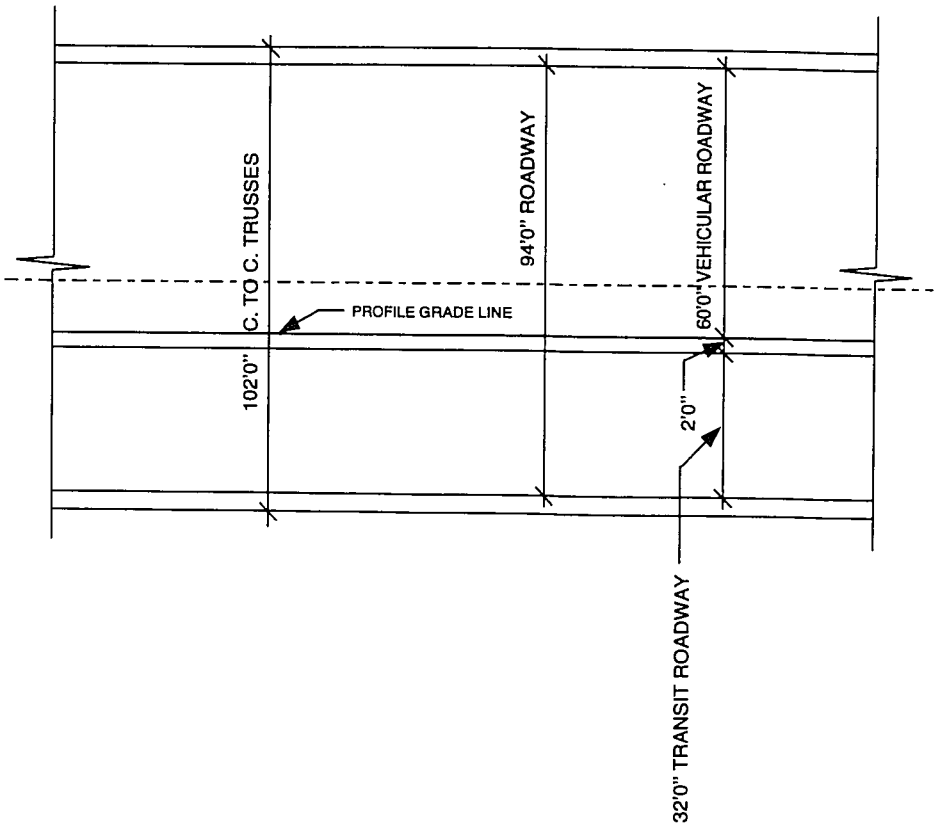

Fig. 3.2-1 Existing Traffic Pattern

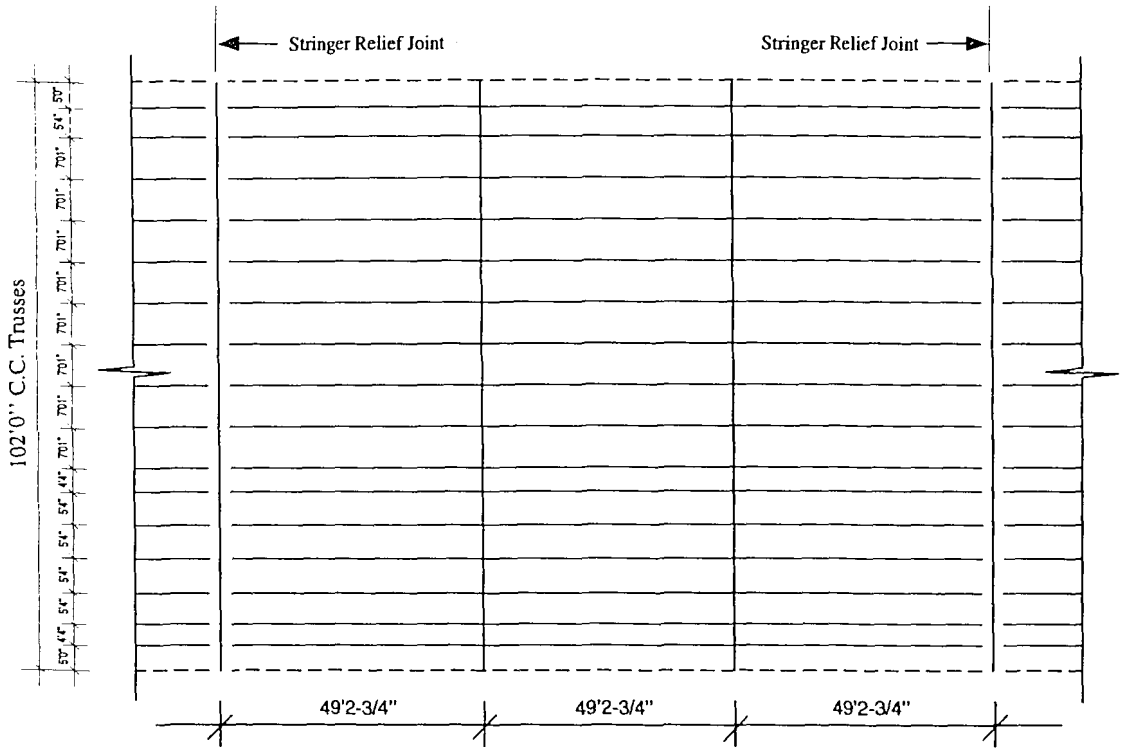

(a) Plan View

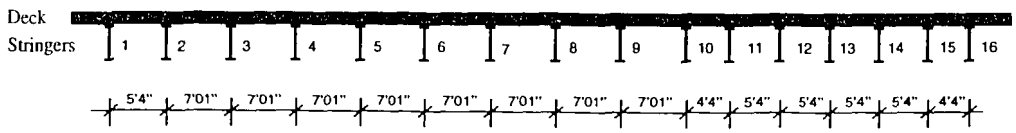

(b) Cross Section

Fig. 4.2-1 Layout of Stringers in Existing Design

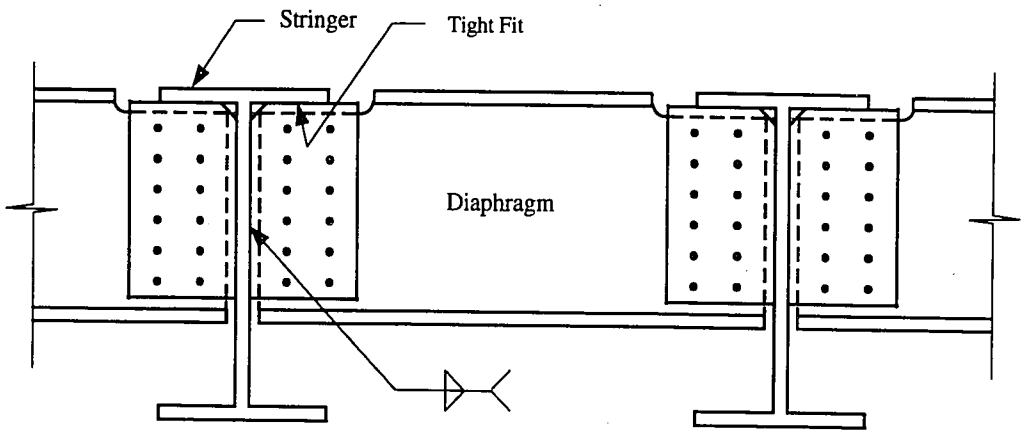

Fig. 4.2-2 Diaphragm-Stringer Connection Detail

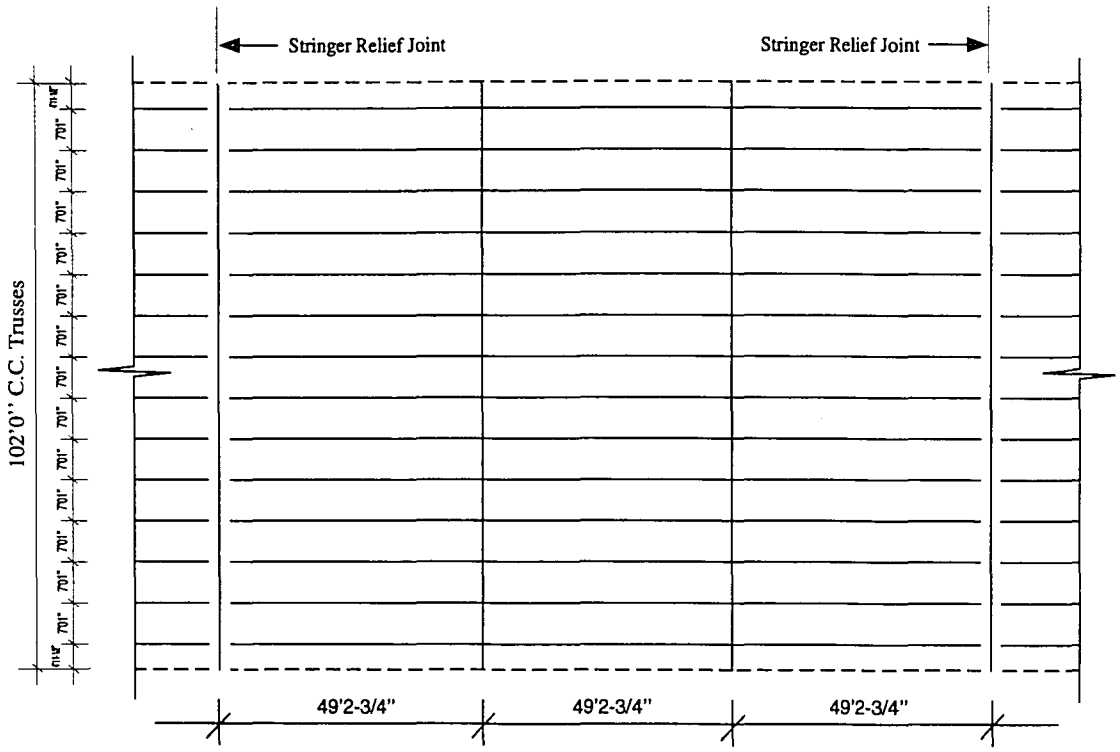

(a) Plan View

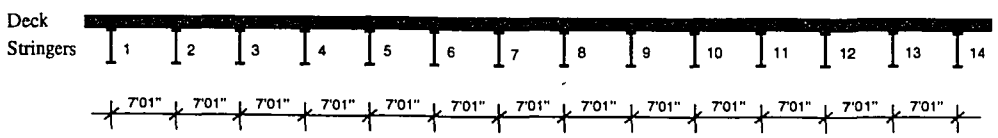

(b) Cross Section

Fig. 4.3-1 Layout of Stringers in Redesign

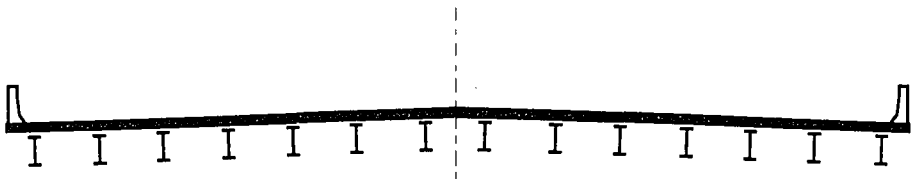

(a) Transverse Direction

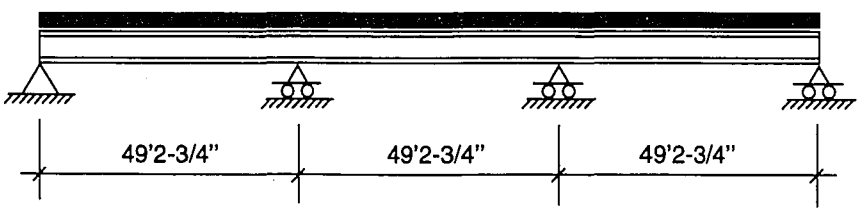

(b) Longitudinal Direction

Fig. 4.4-1 Analysis Model for Stringer Analysis

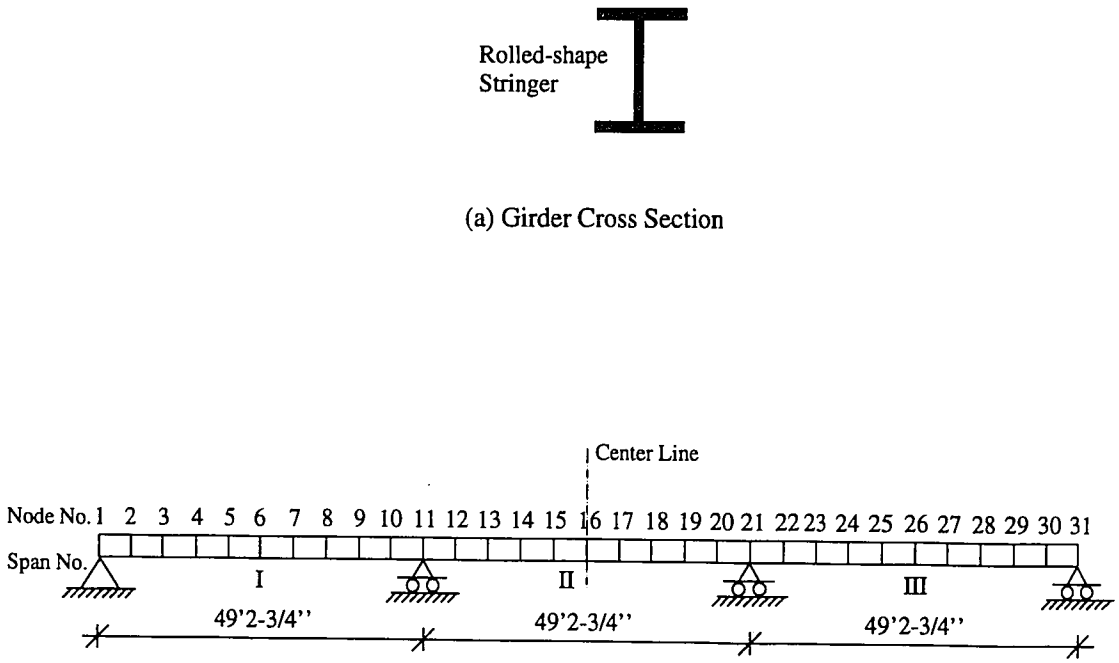

(a) Girder Cross Section

(b) Discretized Analysis Model for Three Span Continuous Stringers

Fig. 4.4-2 Stringer Analysis Using the Girder Analysis Program

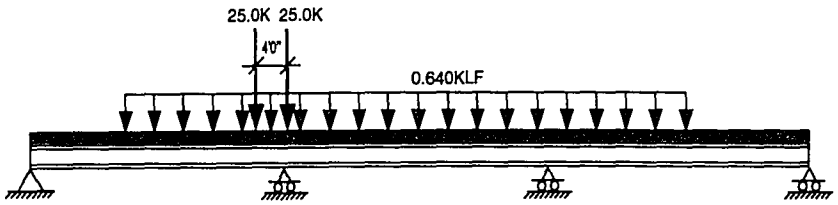

(i) Design Lane Load + Design Tandem

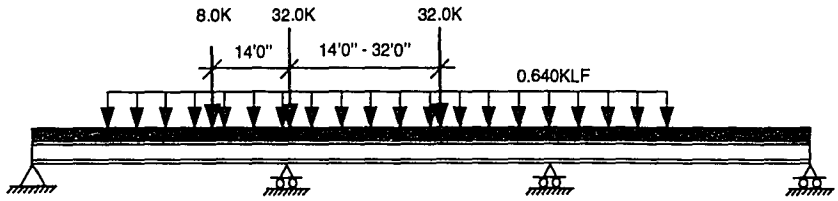

(ii) Design Lane Load + Design Truck

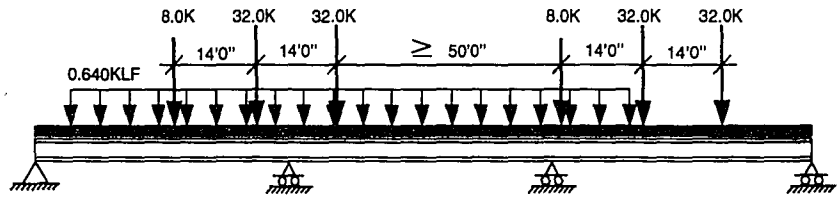

(iii) Design Lane Load + Two Design Trucks

(a) Strength Limit State and Service Limit State

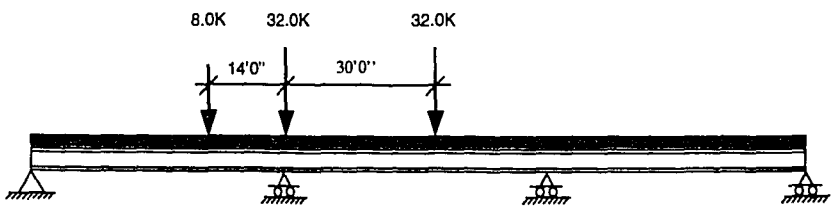

Fatigue Design Truck

(b) Fatigue Limit State

Fig. 4.4-3 LRFD Live Load Combinations for Stringer Design

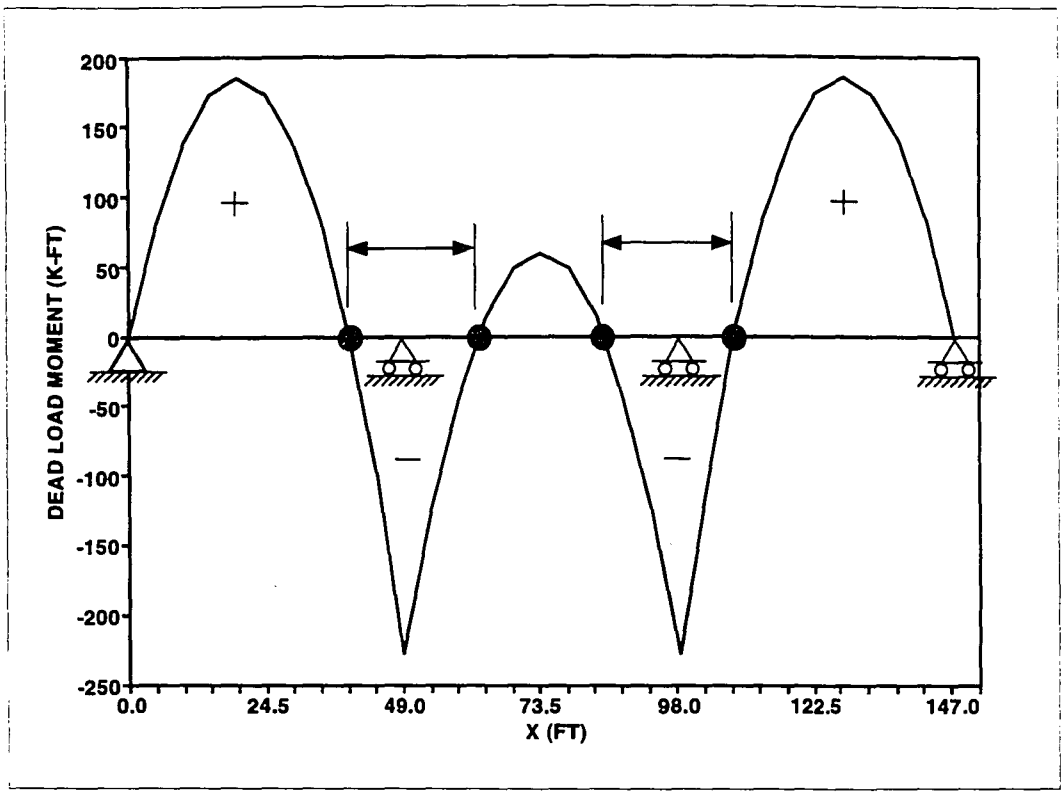

● Dead Load Moment Contraflexure Points

⟷ Needs Consideration of Two Truck Live Load

Fig. 4.4-4 Application of LRFD's Two Truck Vehicular Live Load

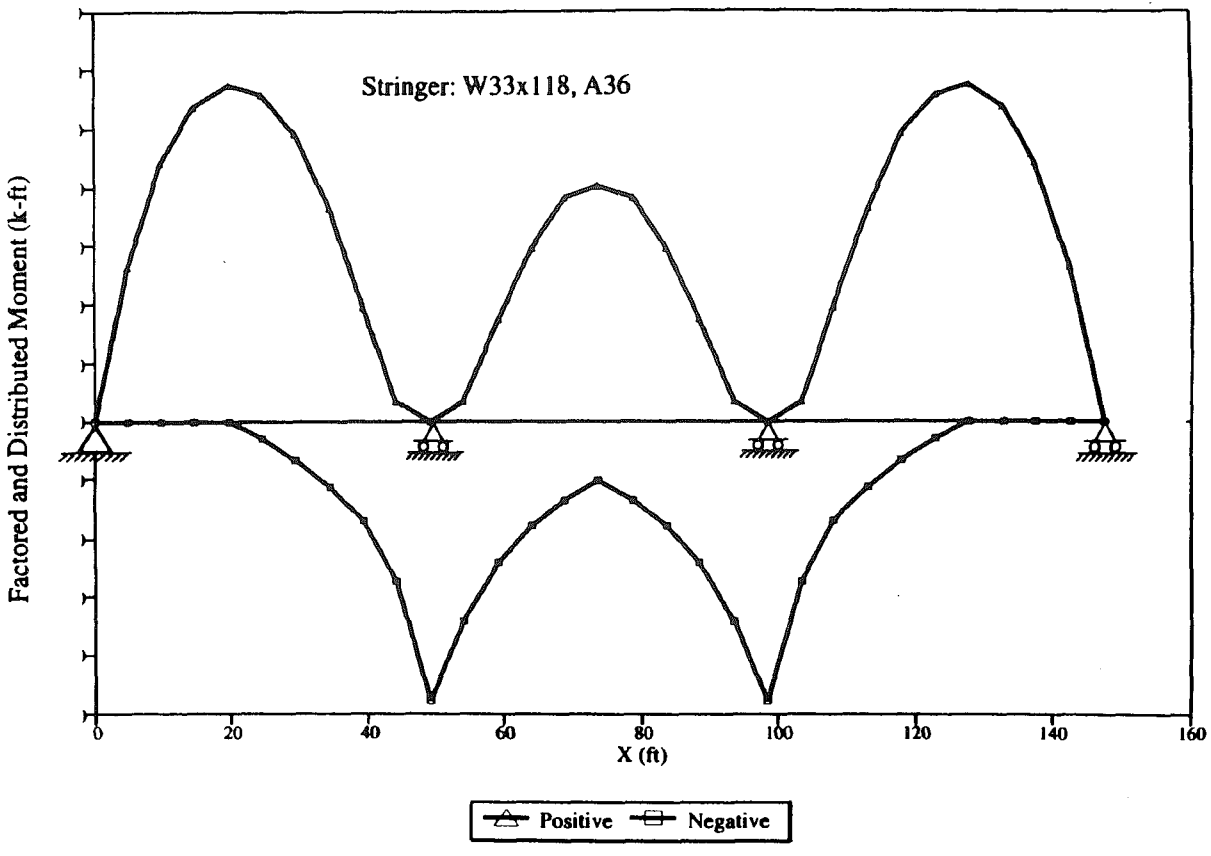

Fig. 4.5-1 Stringer Moment Envelopes
for Strength Limit State

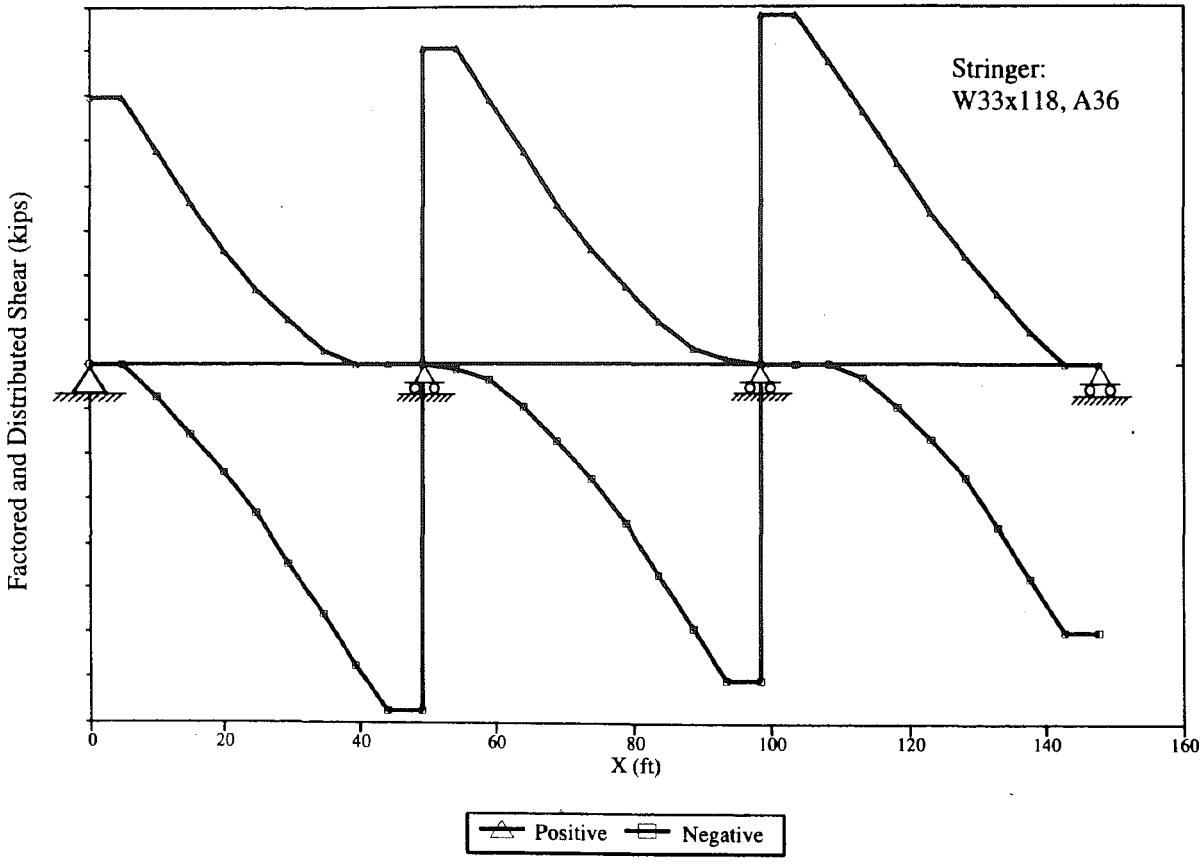

Fig. 4.5-2 Stringer Shear Envelopes
for Strength Limit State

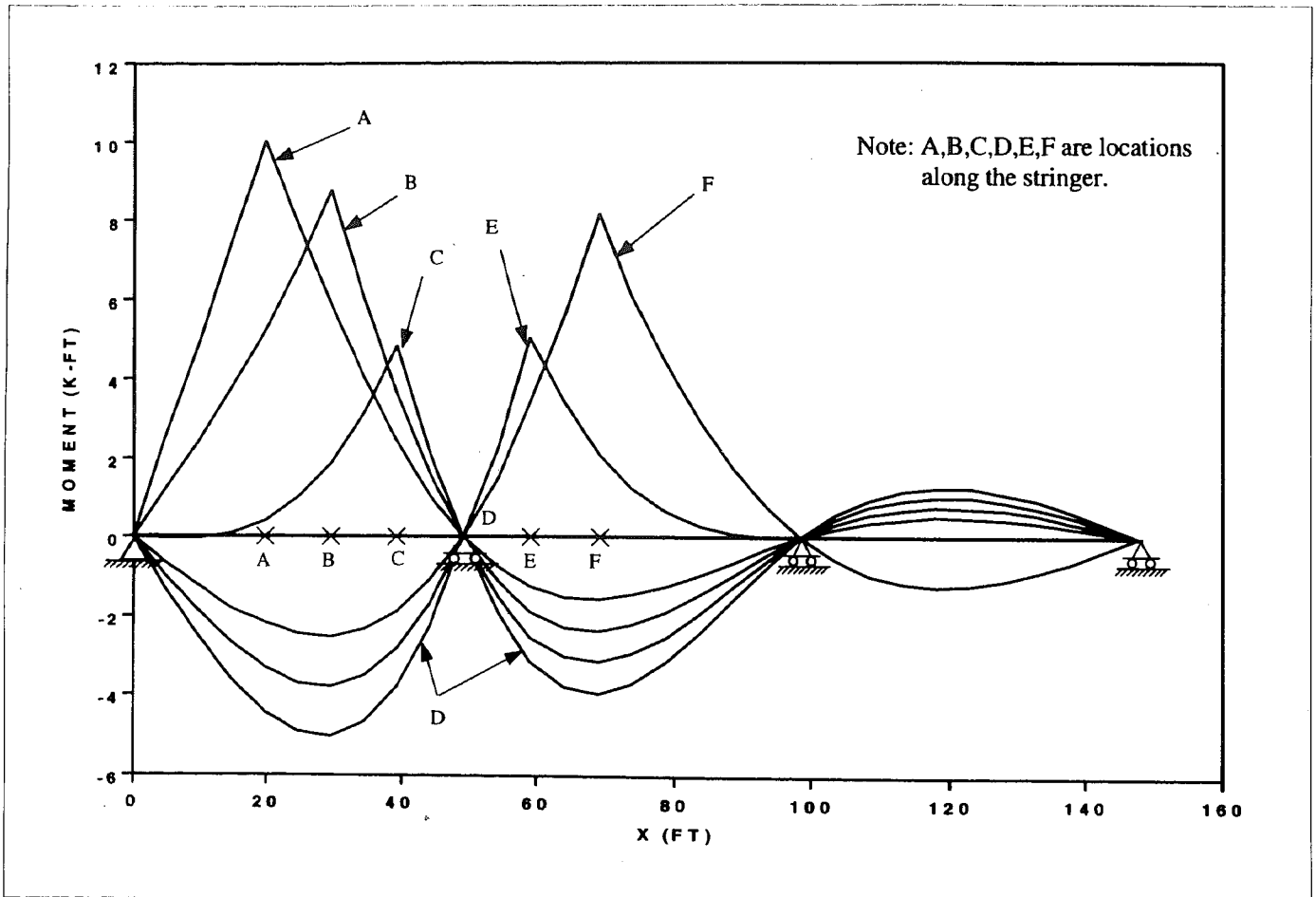

Fig. 4.5-3 Moment Influence Lines for Stringers

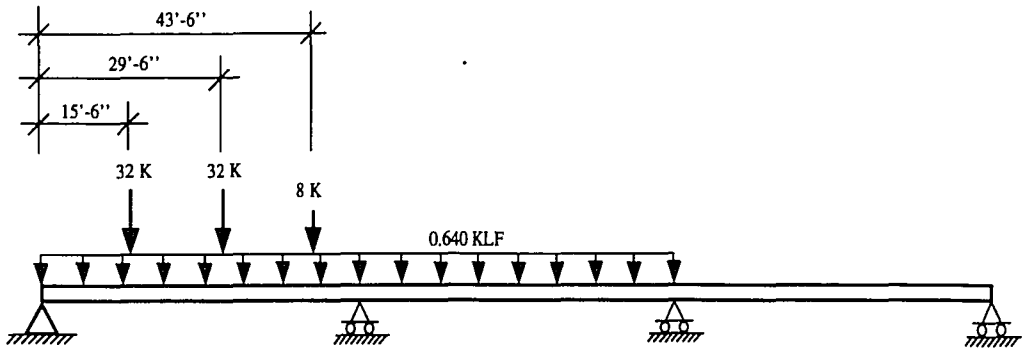

a) Load Case D

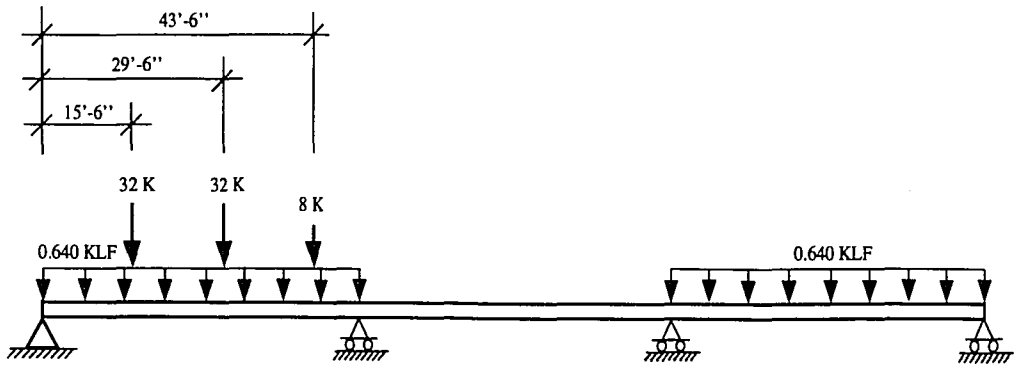

b) Load Case G

Fig. 4.5-4 Critical Load Cases for Negative Moment Design of Stringers

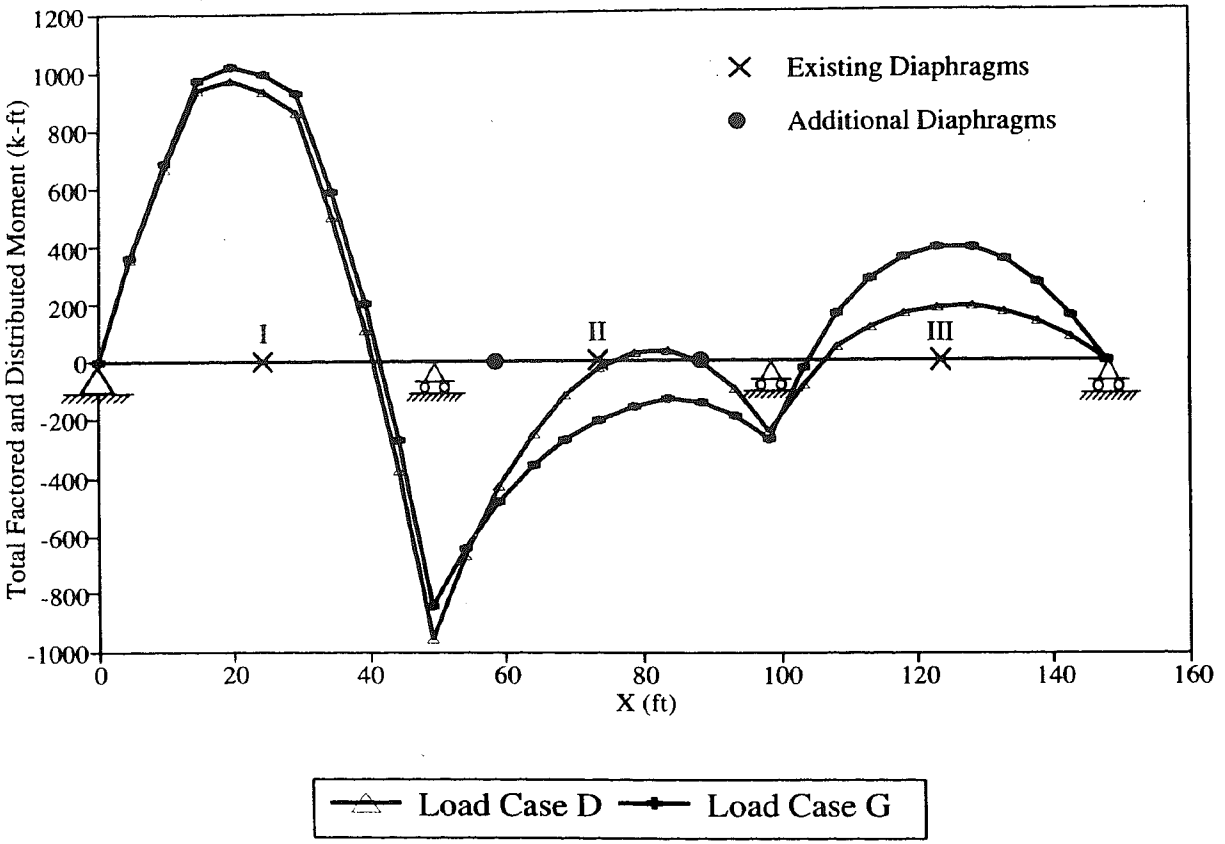

Fig. 4.5-5 Stringer Moment Diagrams for Critical Negative Moment Cases (Strength Limit State)

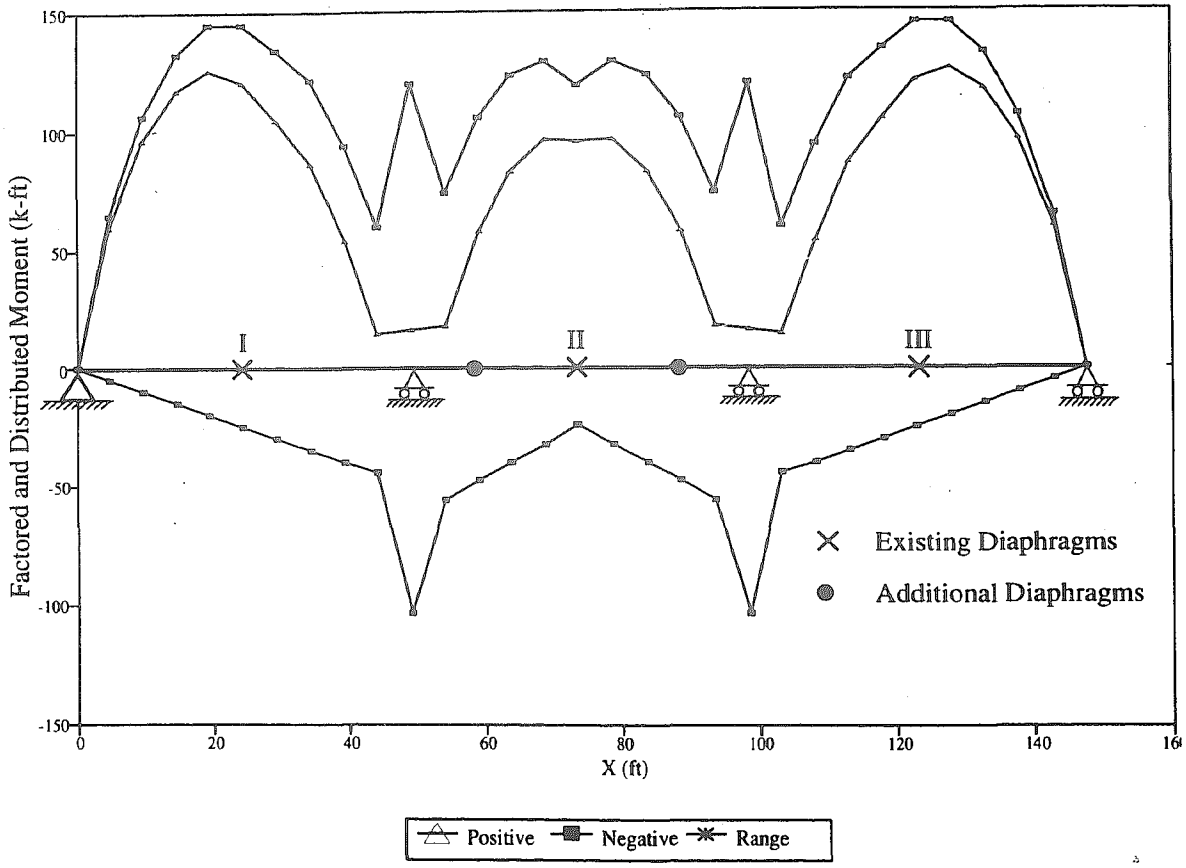

Fig. 4.5-6 Stringer Moment Envelopes for Fatigue Limit State (Live Load Only)

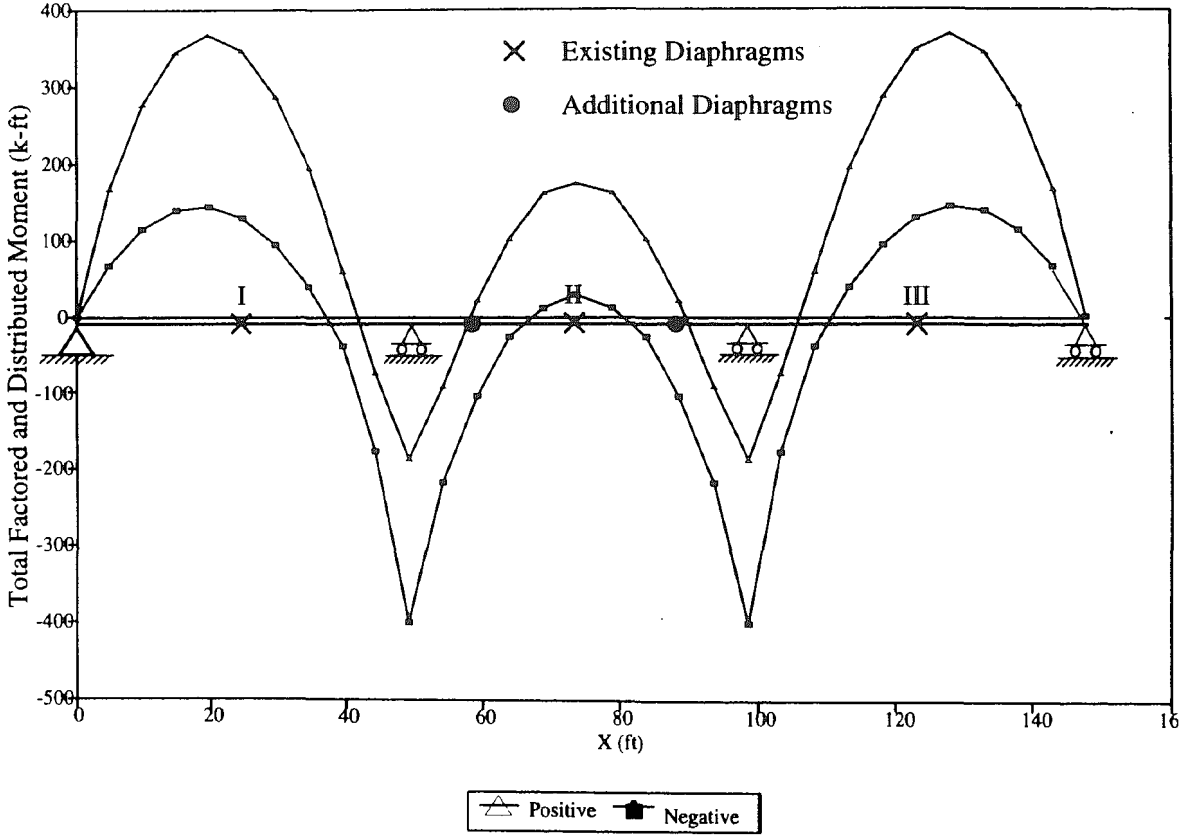

Fig. 4.5-7 Stringer Moment Envelopes for Fatigue Limit State (Live and Dead Load)

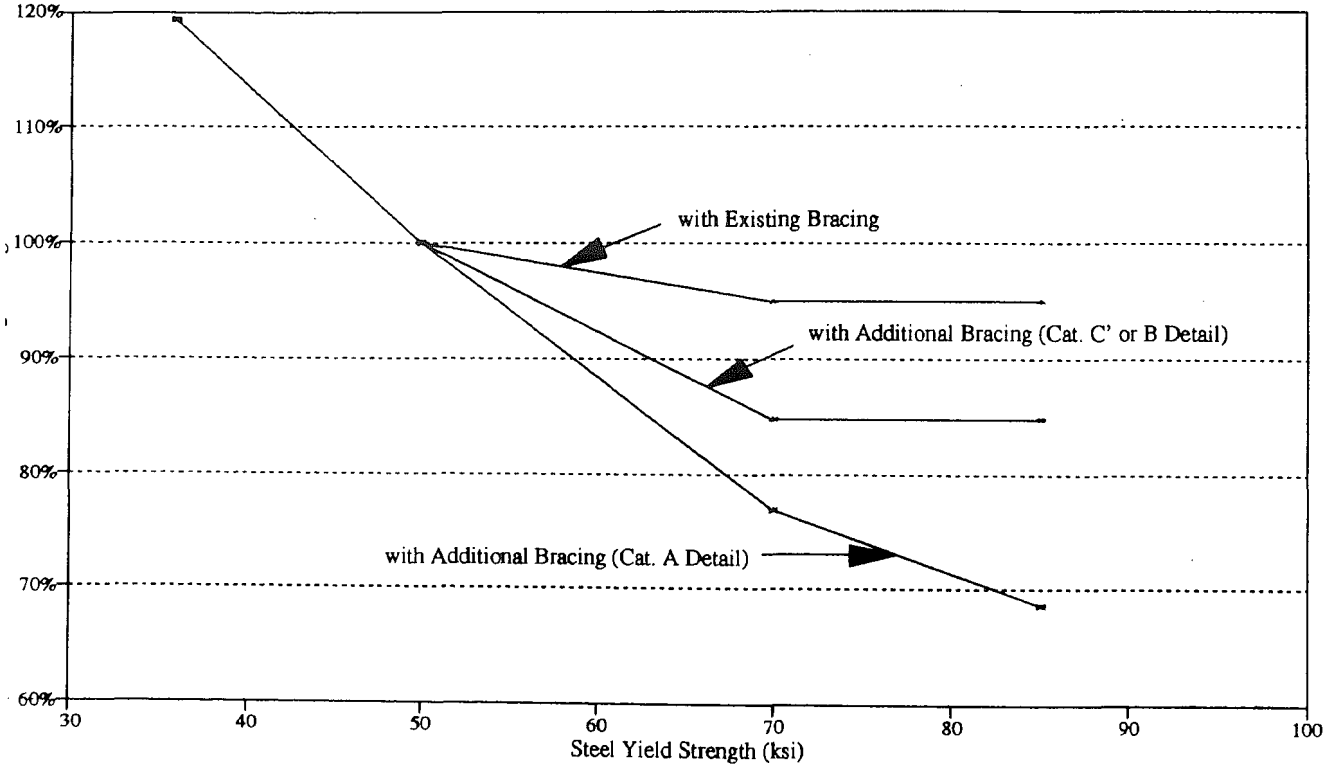

Fig. 4.5-8 Normalized Stringer Weight Versus Steel Yield Strength

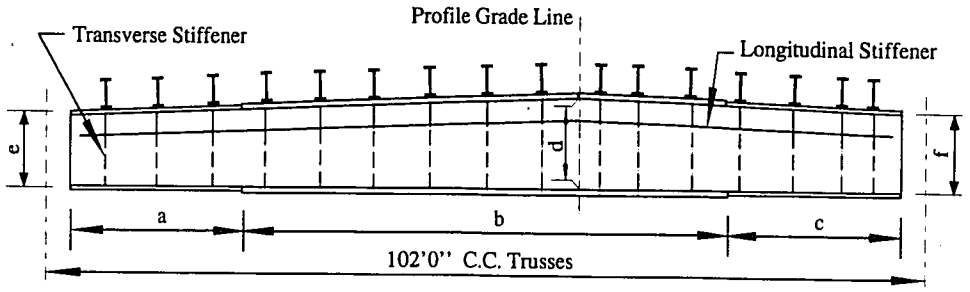

Flange Plate Sizes : a - 1'1/4" x 20'5"
b - 2" x 56'0"
c - 1'1/4" x 22'5"

Web Plate Thickness : 9/16"

Web Plate Depth : d - 10'11-3/4"
e - 9'5"
f - 10'1-7/16"

Fig. 5.2-1 Existing Floor Beam Design in Suspended Span

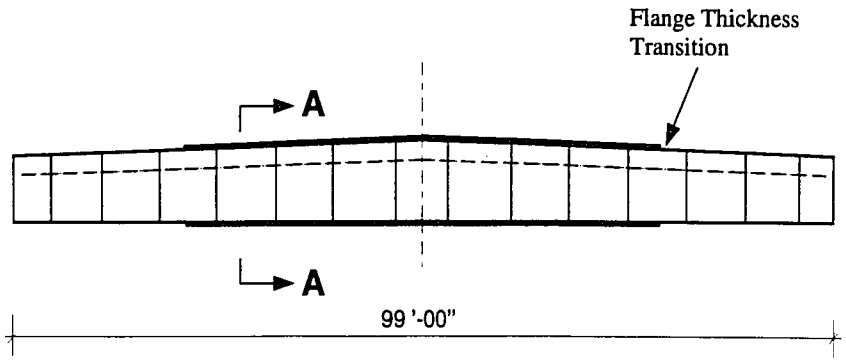

a) Side View

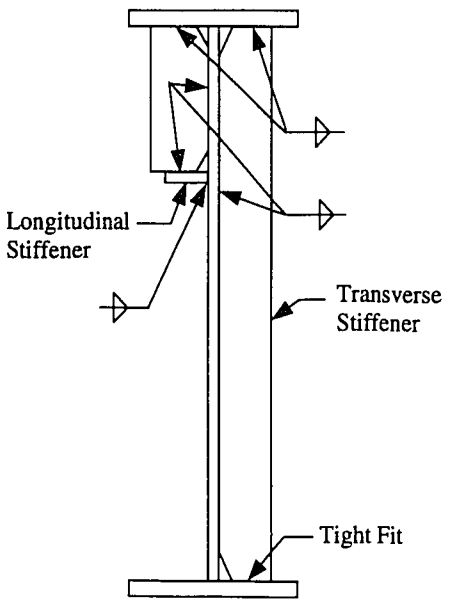

b) Section A-A

Fig. 5.3-1 General Configuration of Floor Beam in Redesign

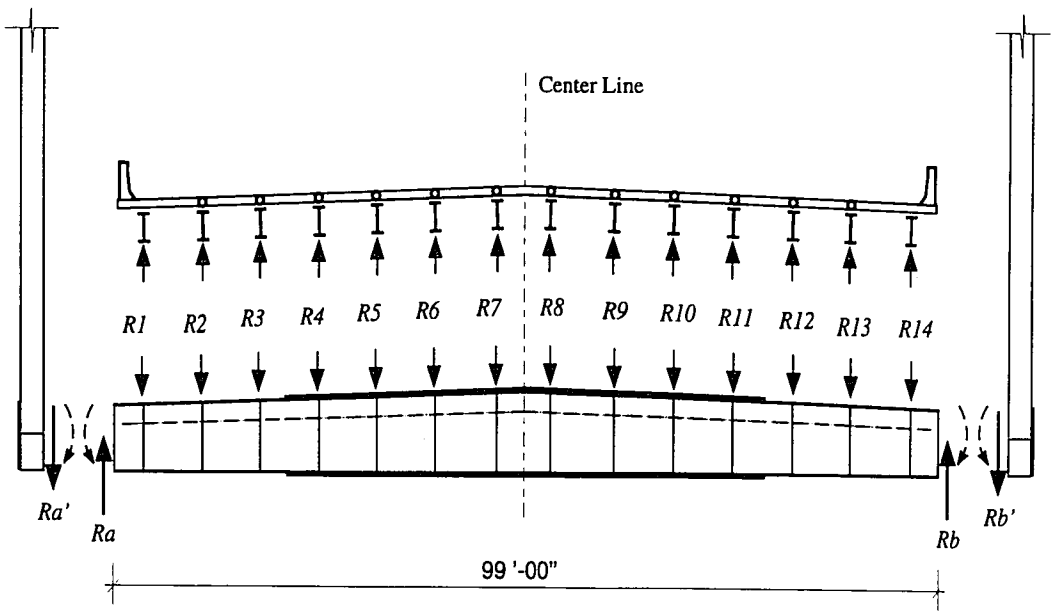

(a) Load Transfer Among Stringers, Floor Beams and Trusses

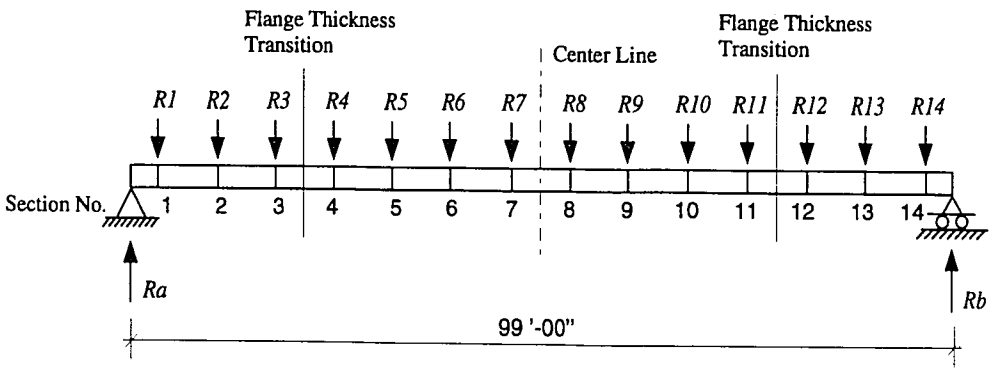

(b) Analysis Model for Floor Beams

Fig. 5.4-1 Floor Beam Analysis

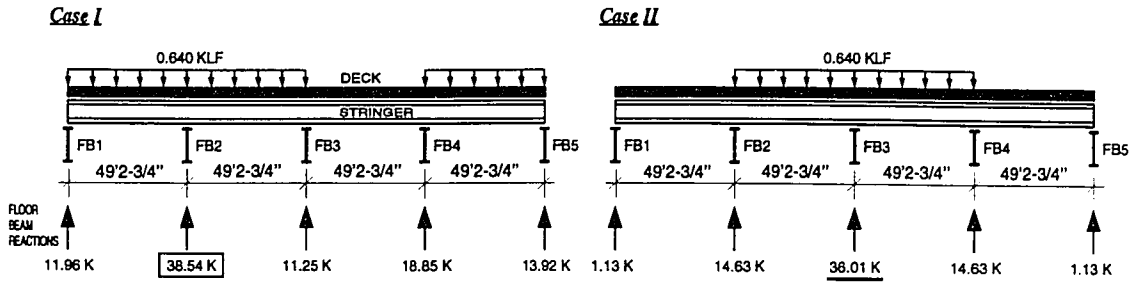

(1) Floor Beams Under Four-span Continuous Stringers

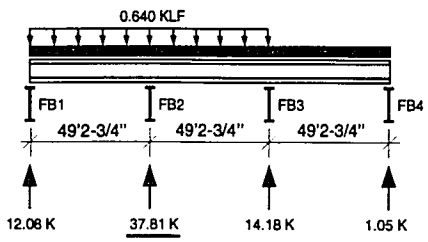

(2) Floor Beams Under Three-span Continuous Stringers

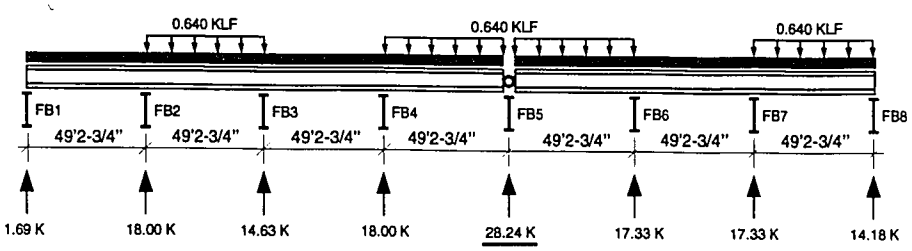

(3) Floor Beams Under Stringer Relief Joints

Maximum stringer reaction under one lane of design lane load = 38.54 kips.

Fig. 5.4-2 Maximum Stringer Reaction on Floor Beams for Design Lane Load

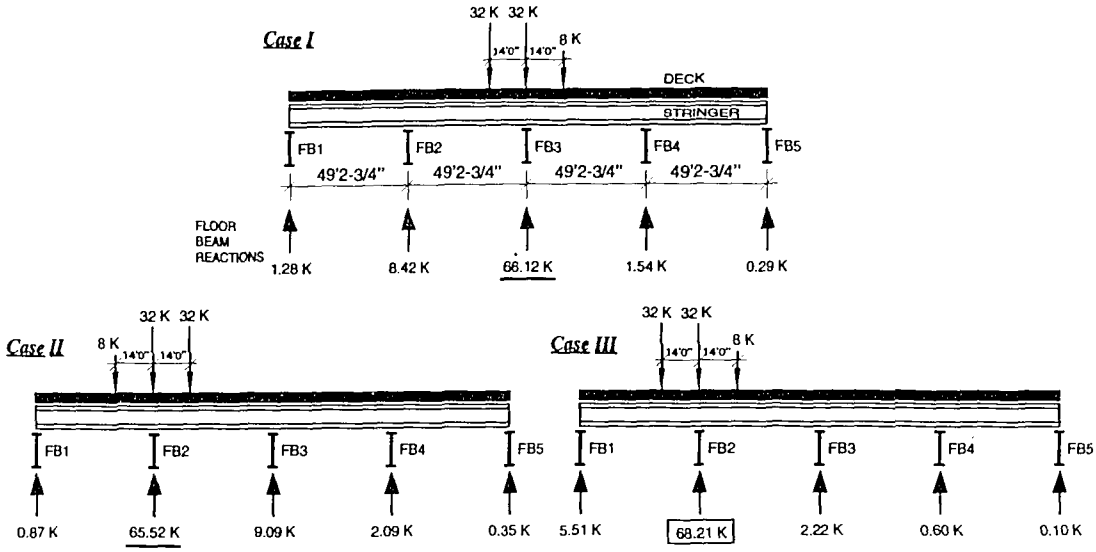

(1) Floor Beams Under Four-span Continuous Stringers

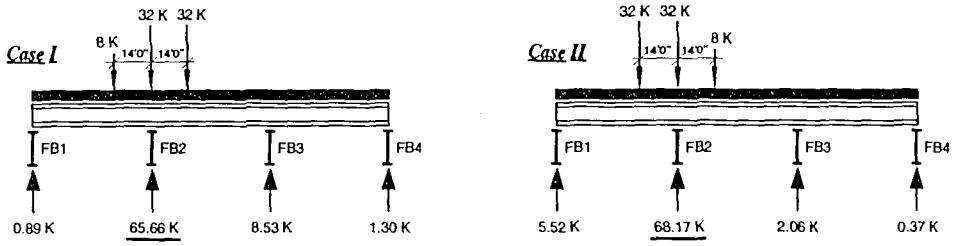

(2) Floor Beams Under Three-span Continuous Stringers

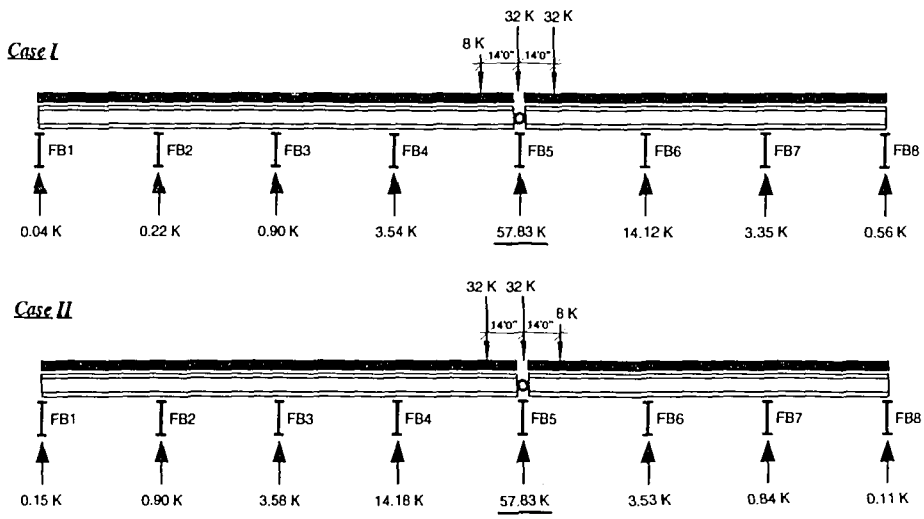

(3) Floor Beams Under Stringer Relief Joints

Maximum stringer reaction under one lane of design truck = 68.21 kips.

Fig. 5.4-3 Maximum Stringer Reaction on Floor Beams for Design Truck

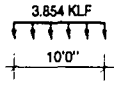

Lane load for transverse distribution converted from maximum stringer reaction due to longitudinal distribution of one lane of design lane load

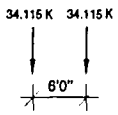

Truck load for transverse distribution converted from maximum stringer reaction due to longitudinal distribution of one lane of design truck

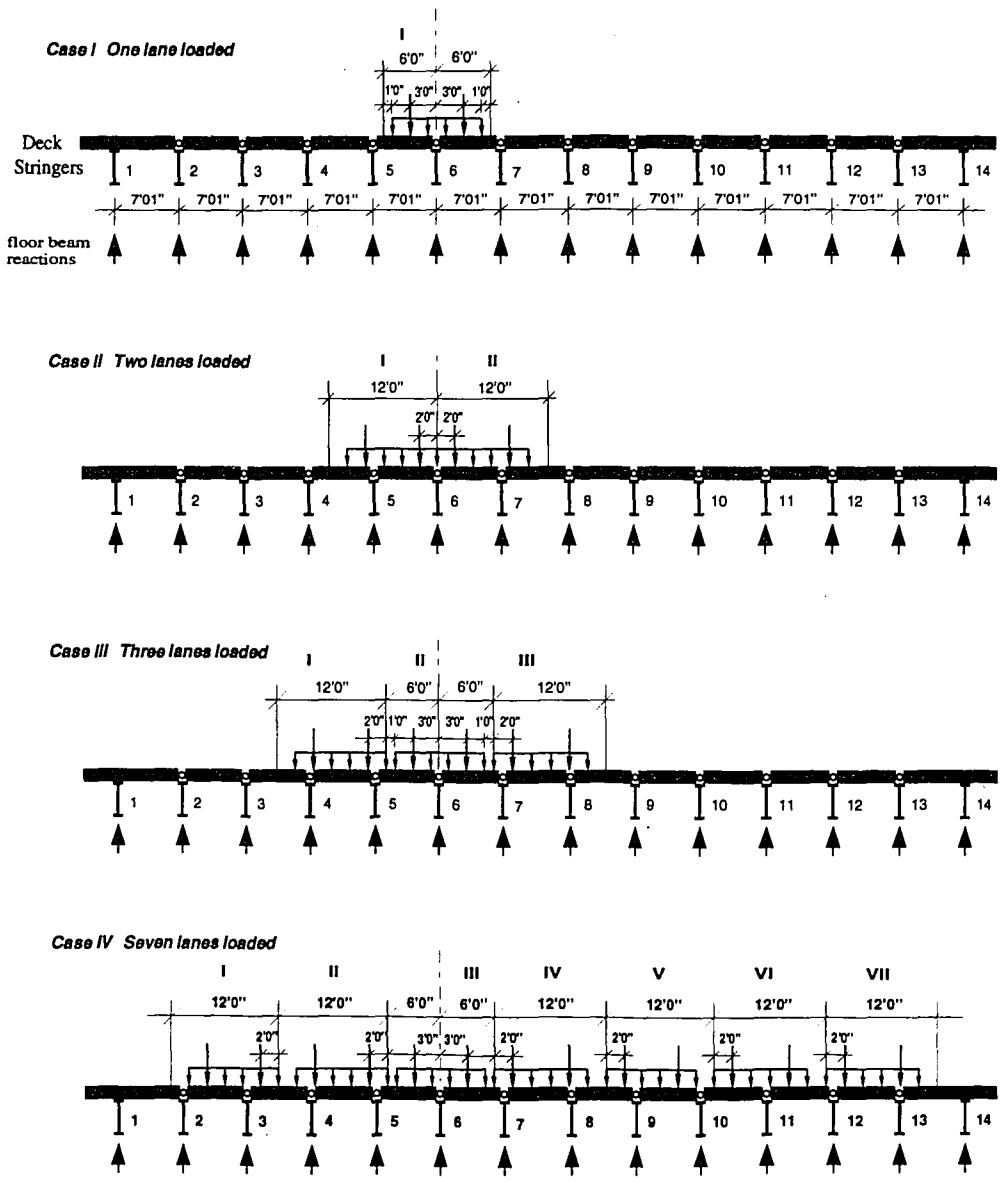

Fig. 5.4-4 Transverse Live Load Positioning for Floor Beam Section No. 6

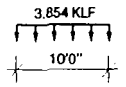

Lane load for transverse distribution converted from maximum stringer reaction due to longitudinal distribution of one lane of design lane load

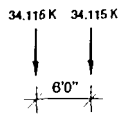

Truck load for transverse distribution converted from maximum stringer reaction due to longitudinal distribution of one lane of design truck

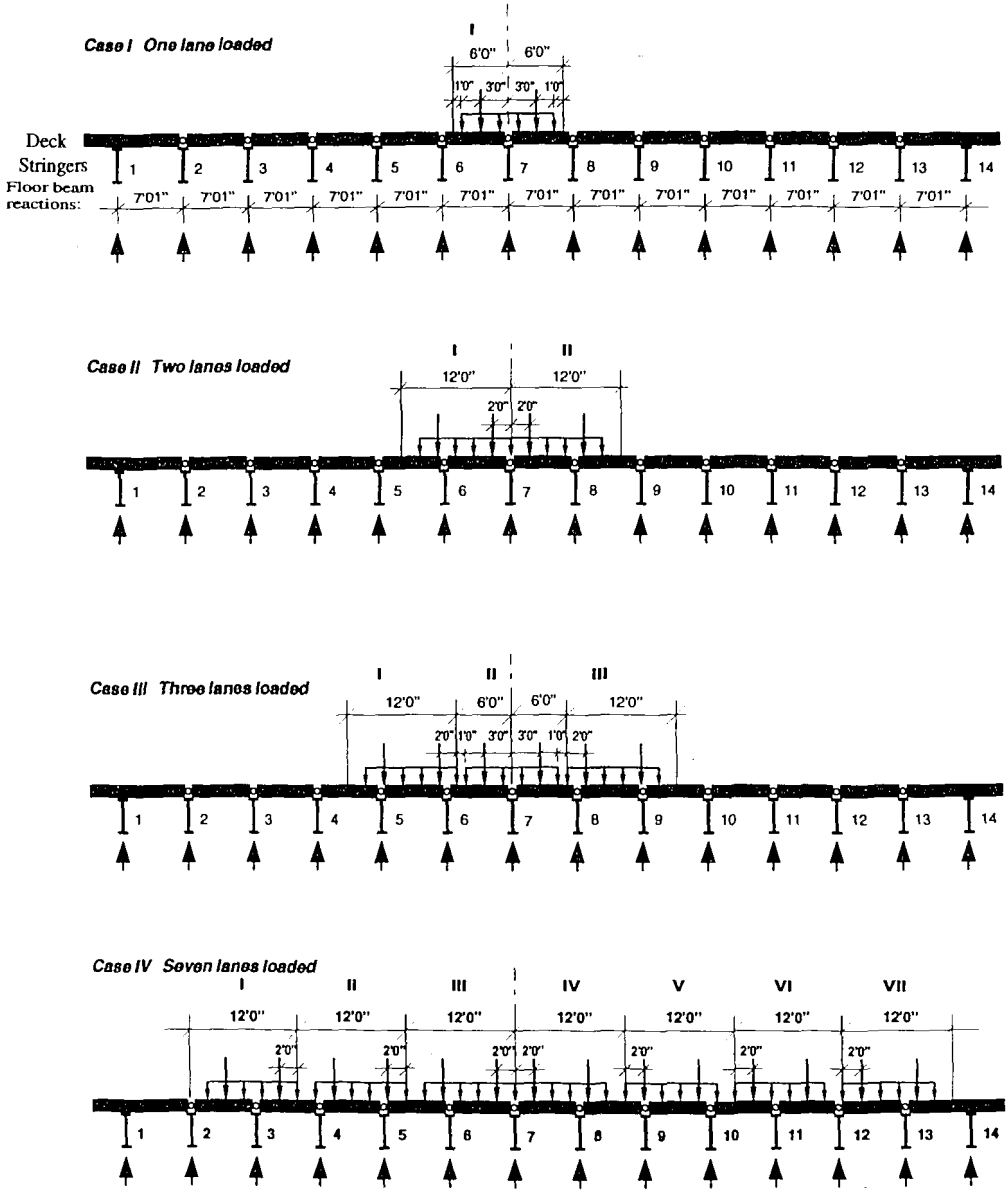

Fig. 5.4-5 Transverse Live Load Positioning for Floor Beam Section No. 7

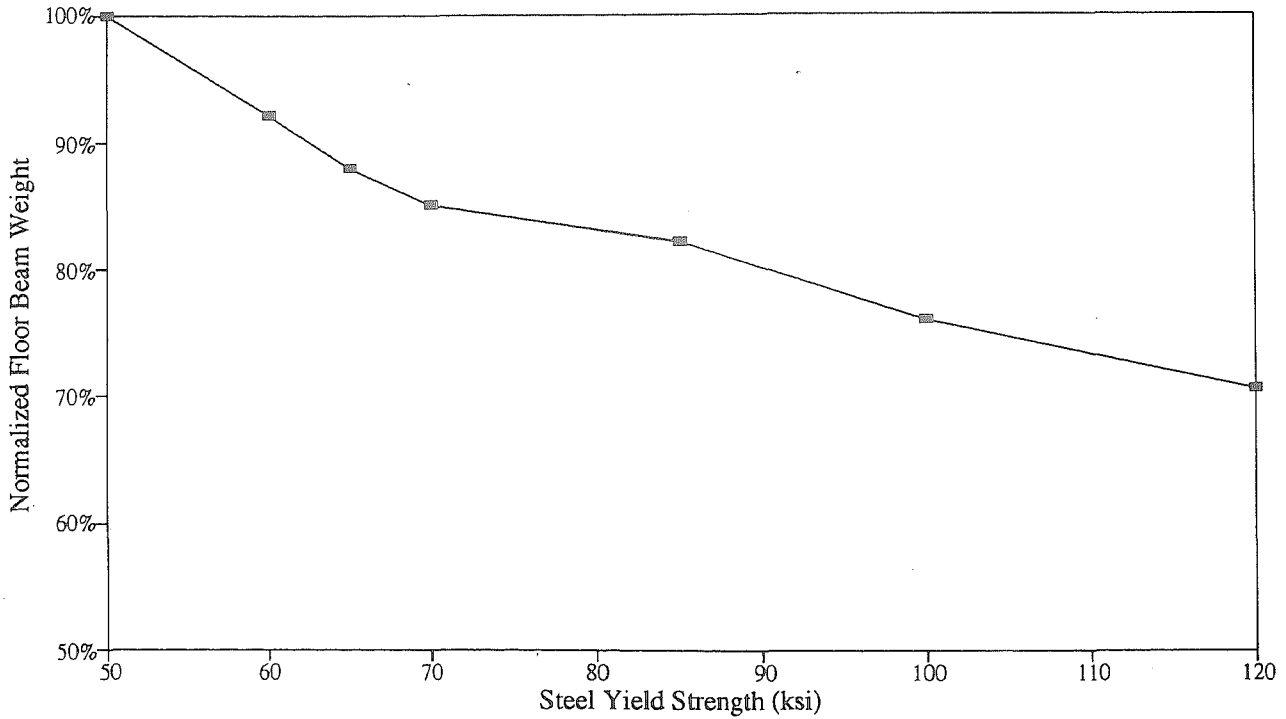

Fig. 5.5-1 Normalized Floor Beam Weight Versus Steel Yield Strength

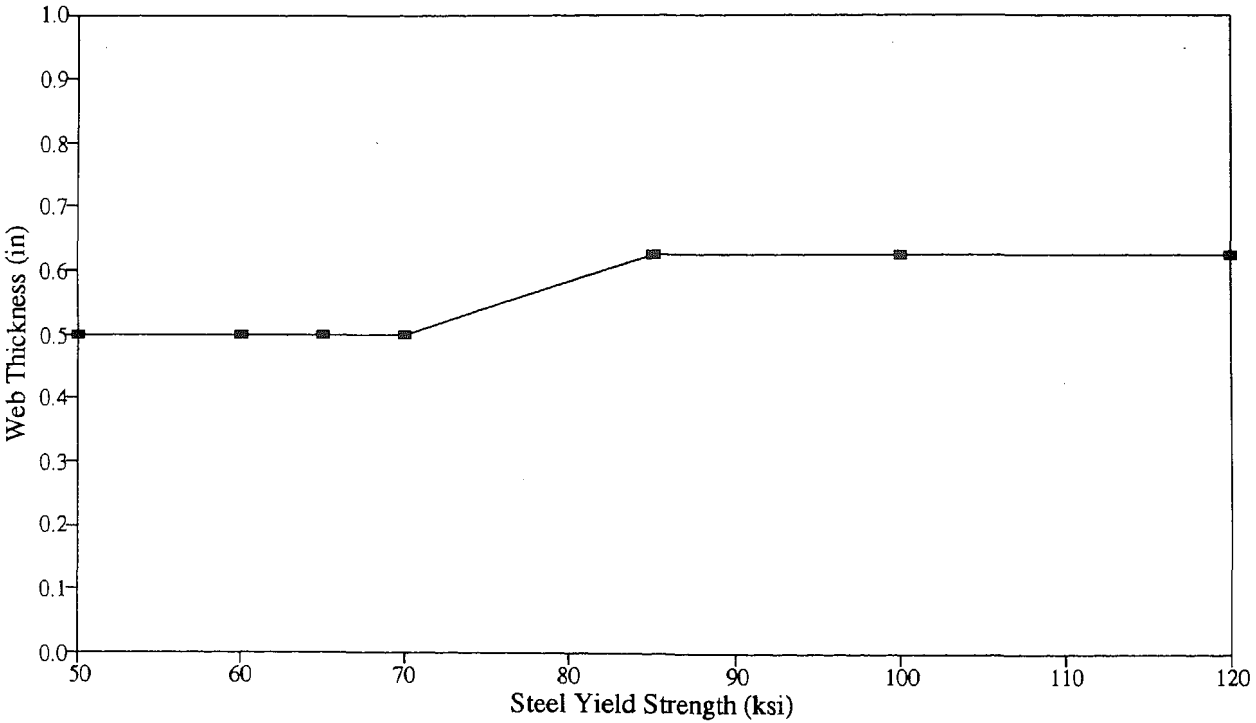

Fig. 5.5-2 Floor Beam Web Thickness Versus Steel Yield Strength

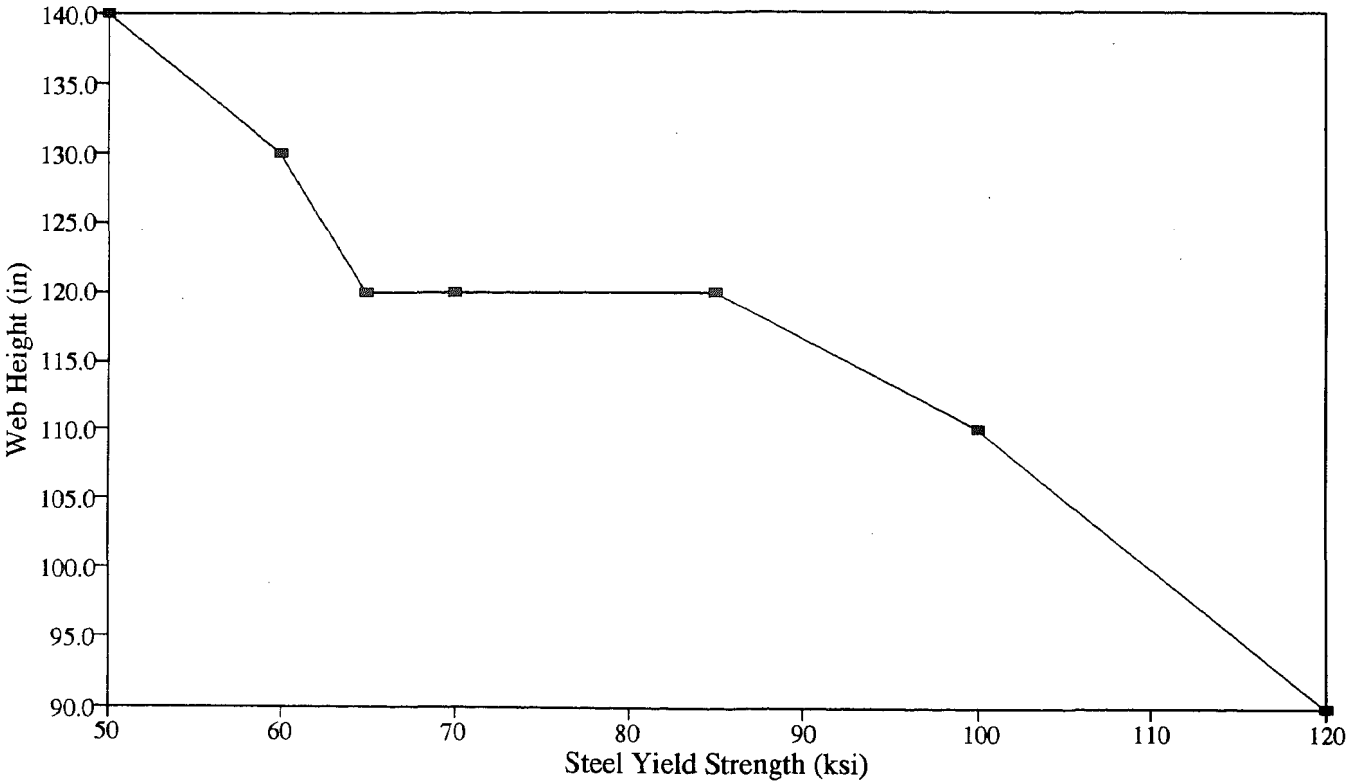

Fig. 5.5-3 Floor Beam Web Height Versus Steel Yield Strength

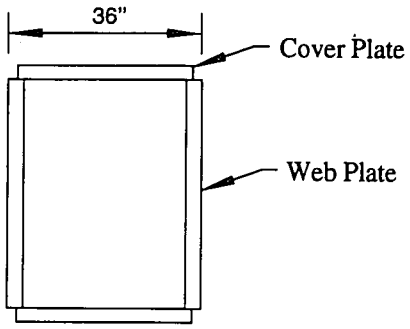

(a) Member Type I

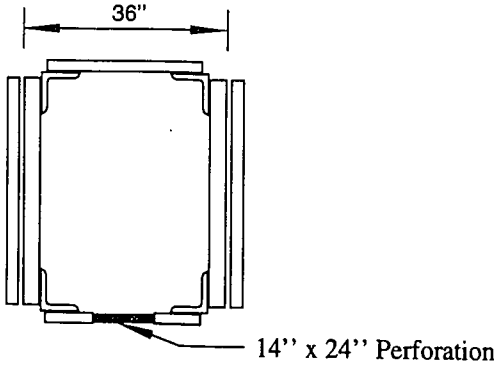

(b) Member Type II

Fig. 6.2-1 Types of Truss Members

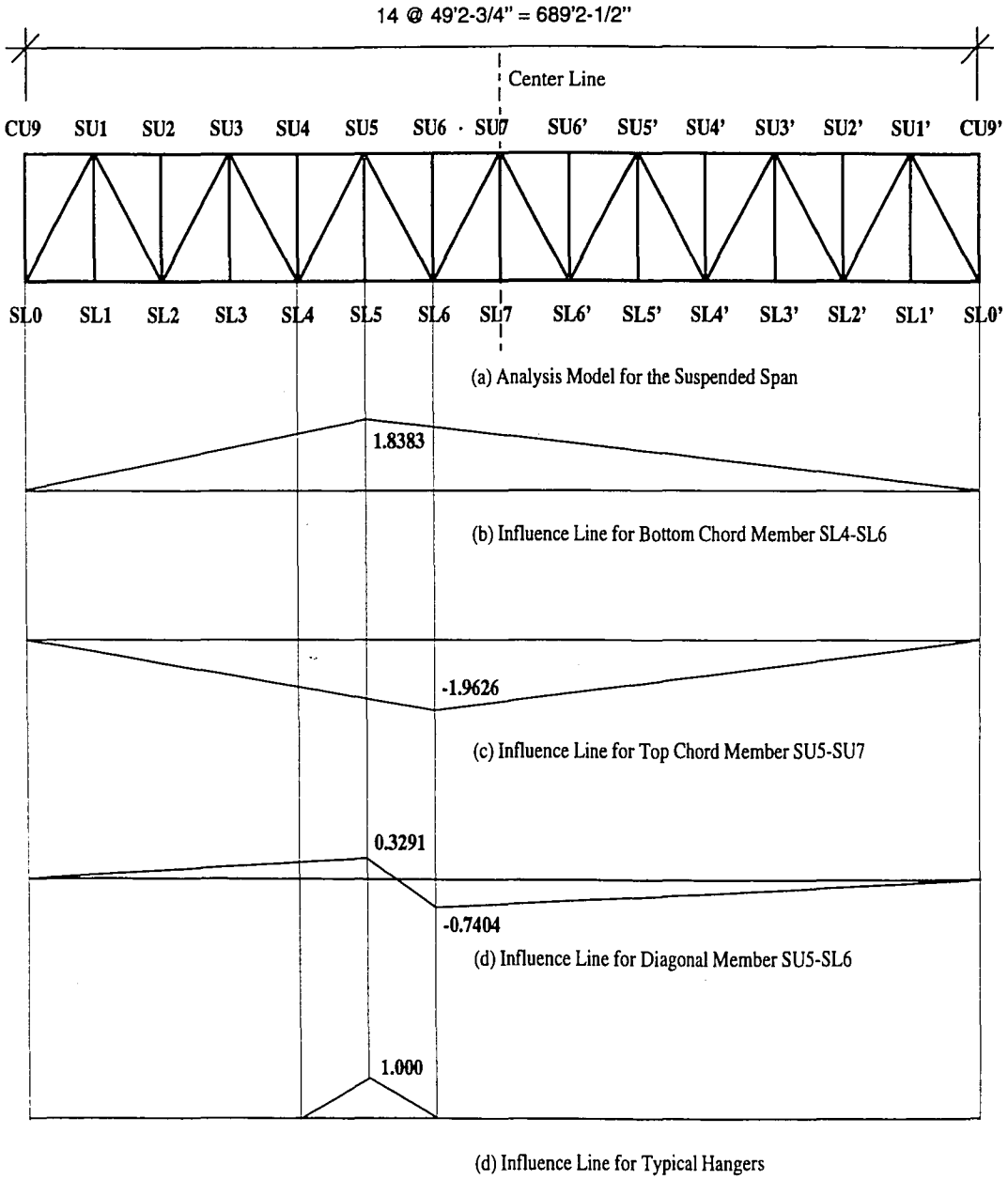

Fig. 6.3-1 Axial Force Influence Lines for Truss Members in Suspended Span

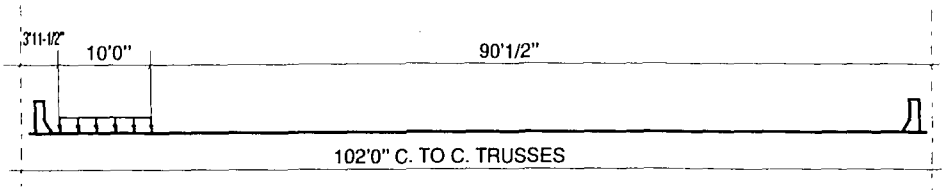

No. of Lanes = [93'1/2'' / 102'0''] x 1.20 = 1.095

(a) One Lane Loaded (MPF = 1.20)

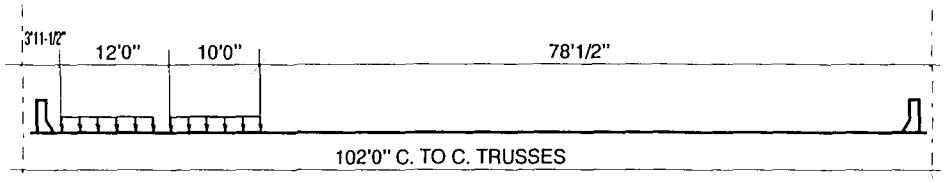

No. of Lanes = [(81'1/2''+93'1/2'') / 102'0''] x 1.00 = 1.707

(b) Two Lanes Loaded (MPF = 1.00)

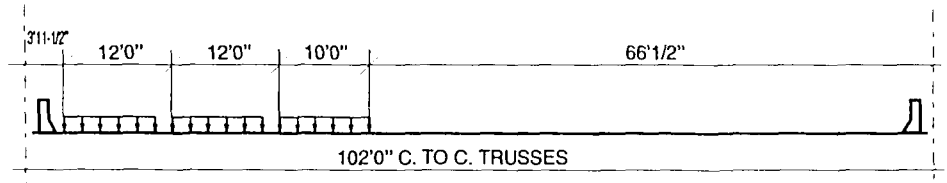

No. of Lanes = [(69'1/2''+81'1/2''+93'1/2'') / 102'0''] x 0.85 = 2.025

(c) Three Lanes Loaded (MPF = 0.85)

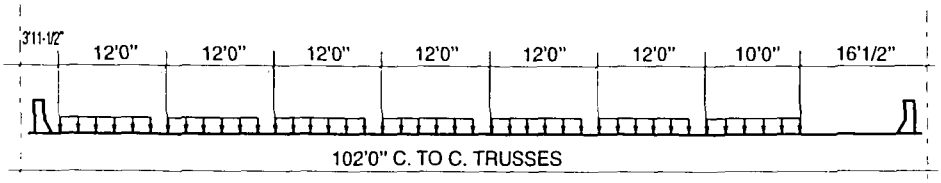

No. of Lanes = [(21'1/2''+33'1/2''+45'1/2''+57'1/2''+69'1/2''+81'1/2''+93'1/2'')/ 102'0''] x 0.65 = 2.545

(d) Seven Lanes Loaded (MPF = 0.65)

Fig. 6.3-2 Equivalent Number of Lanes for Truss Design

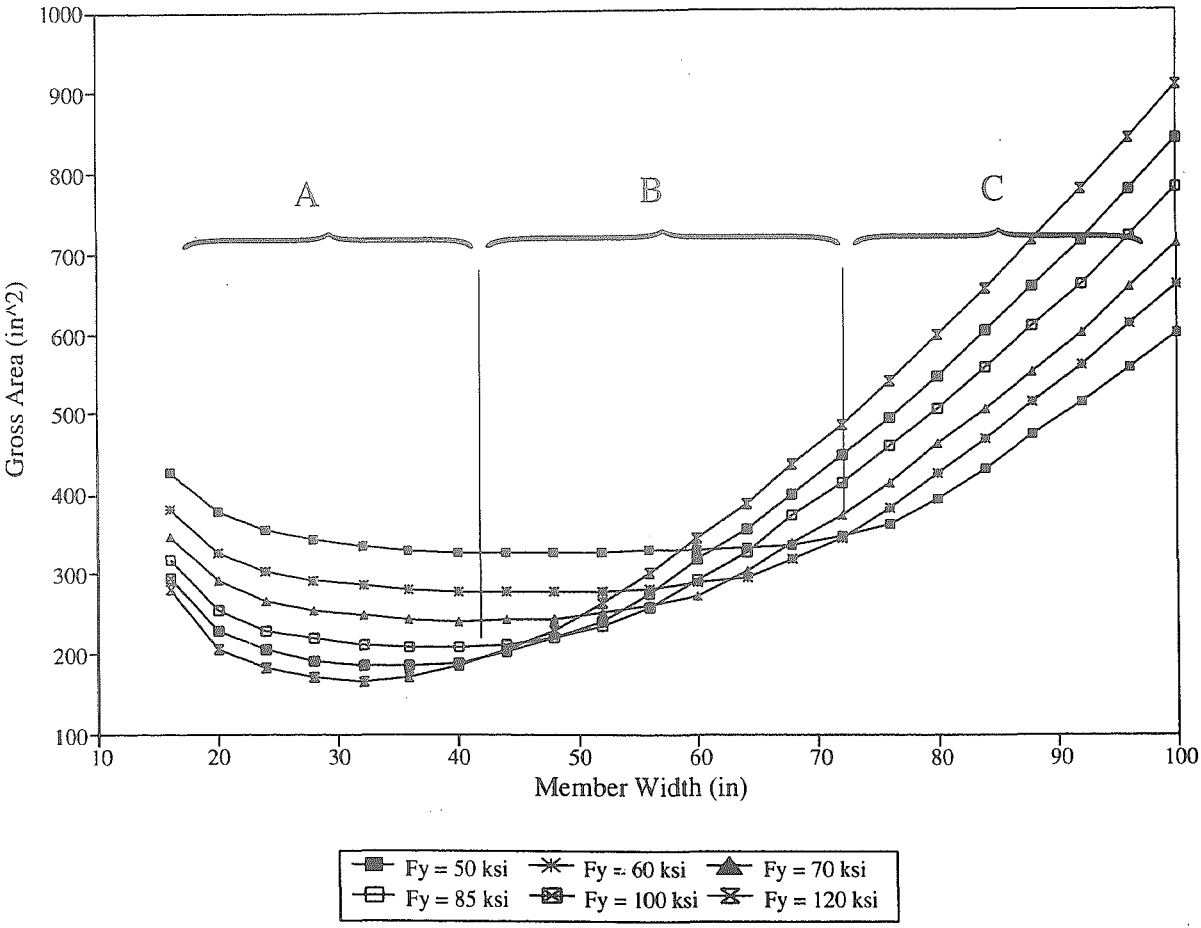

Fig. 6.4-1 Gross Area of Minimum Weight Design Versus Member Width Constraint for Top Chord SU5-SU7

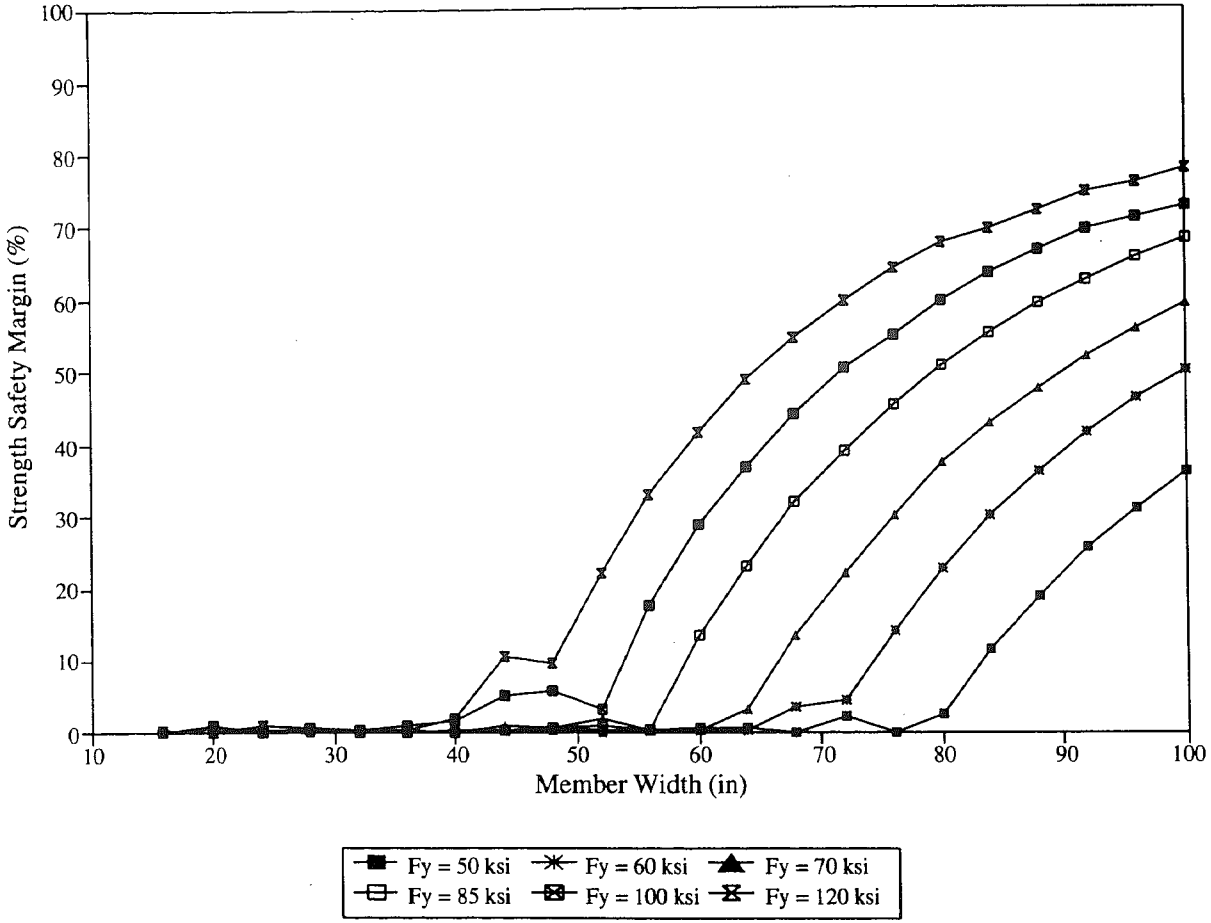

Fig. 6.4-2 Strength Safety Margin of Minimum Weight Design Versus Member Width Constraint for Top Chord SU5-SU7

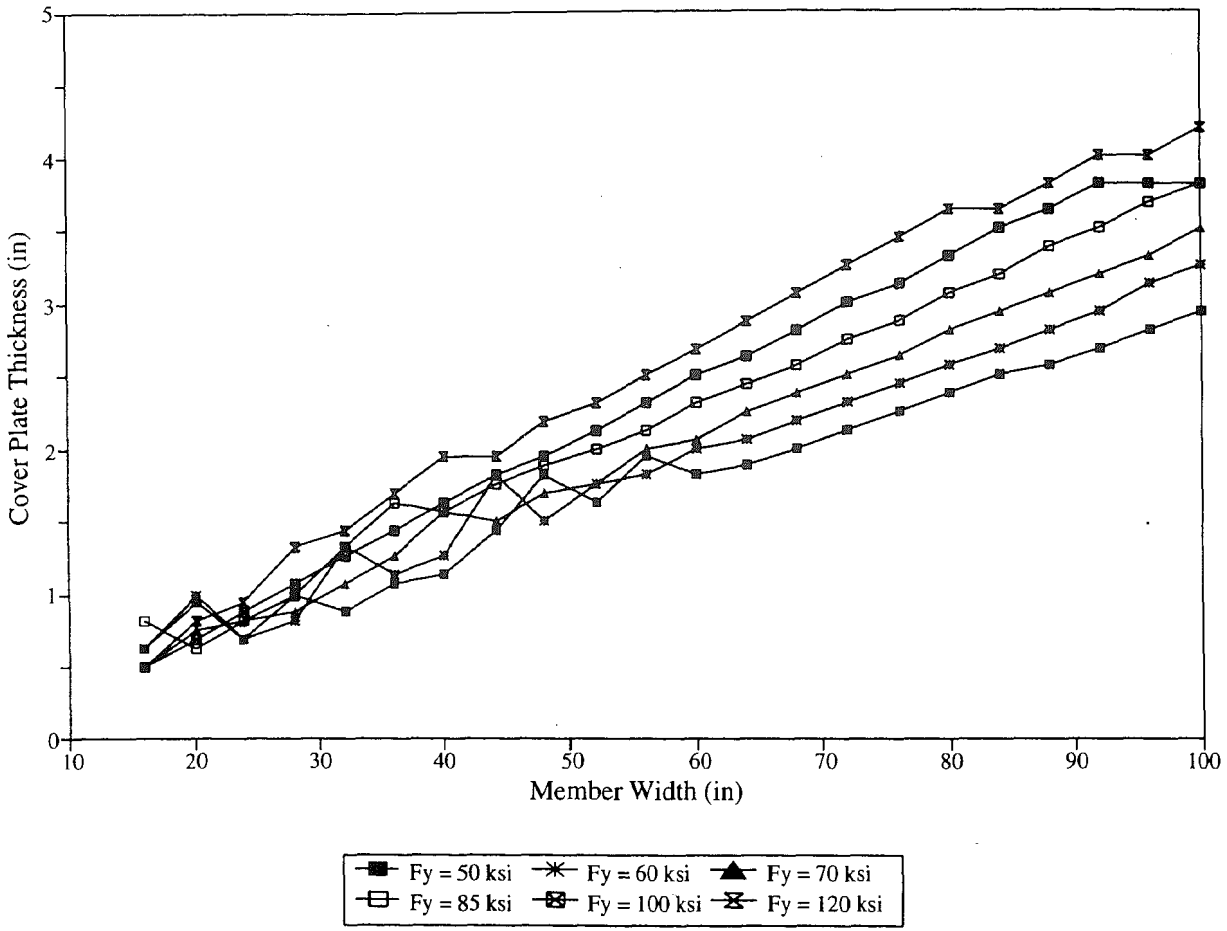

Fig. 6.4-3 Cover Plate Thickness of Minimum Weight Design Versus Member Width Constraint for Top Chord SU5-SU7

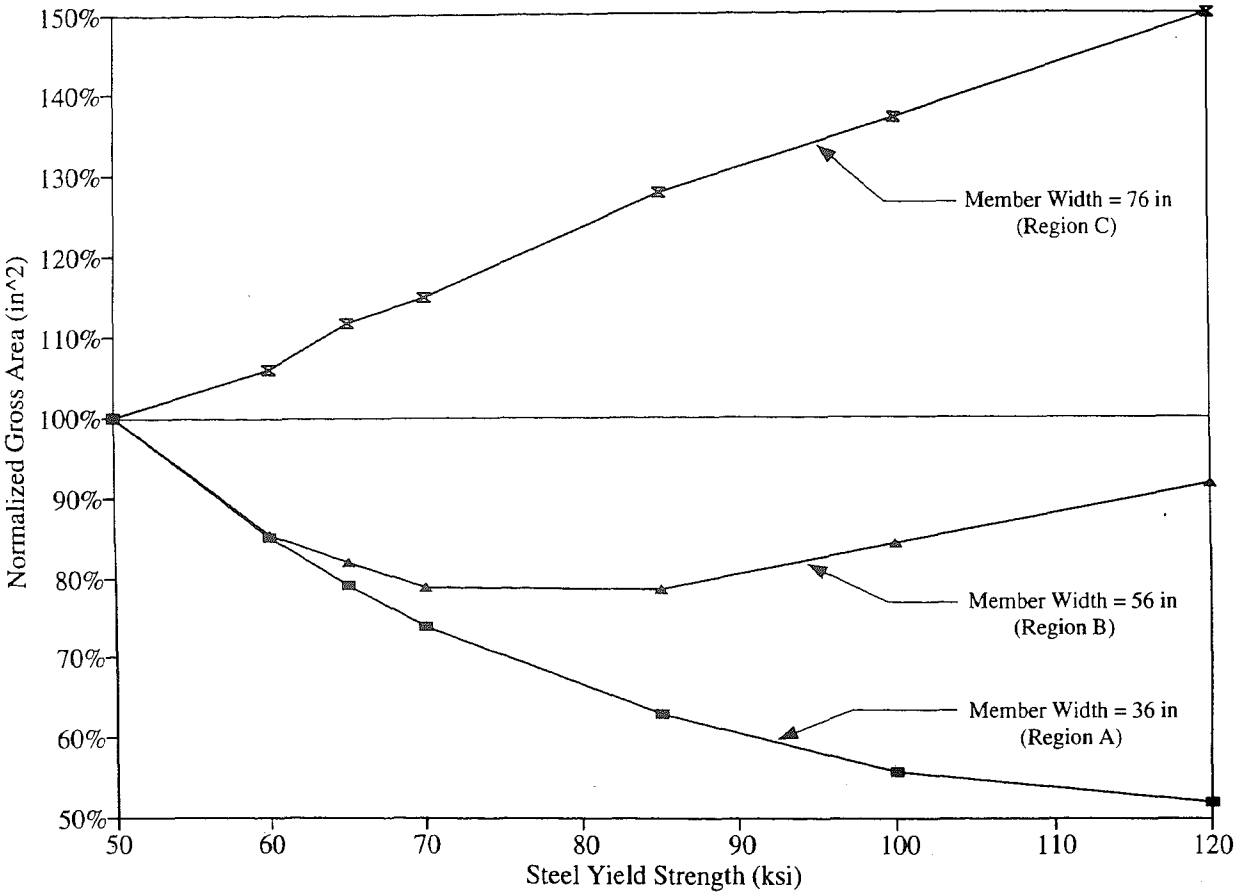

Fig. 6.4-4 Normalized Gross Area of Minimum Weight Design Versus Steel Yield Strength in Different Member Width Regions of Top Chord SU5-SU7

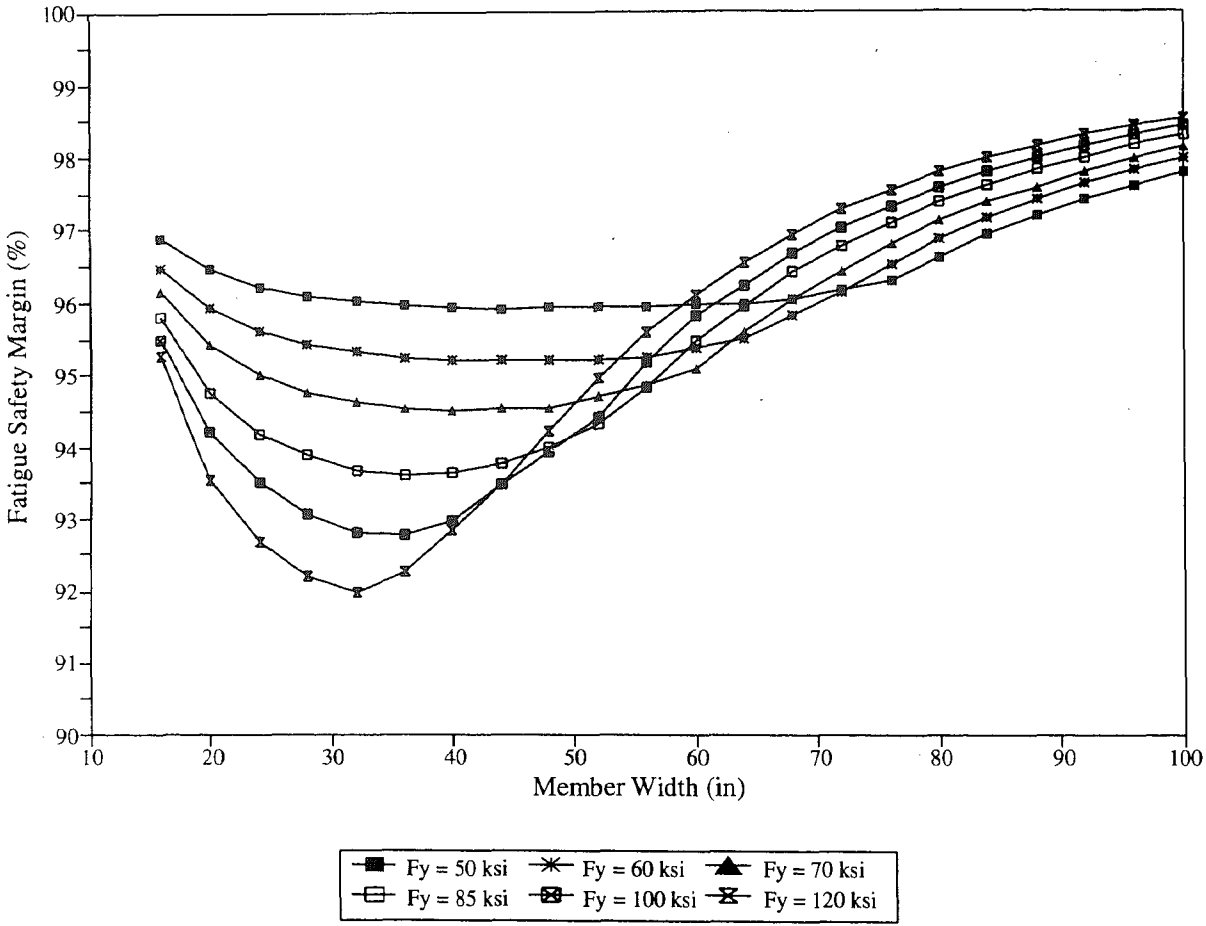

Fig. 6.4-5 Fatigue Safety Margin of Minimum Weight Design Versus Member Width Constraint for Top Chord SU5-SU7

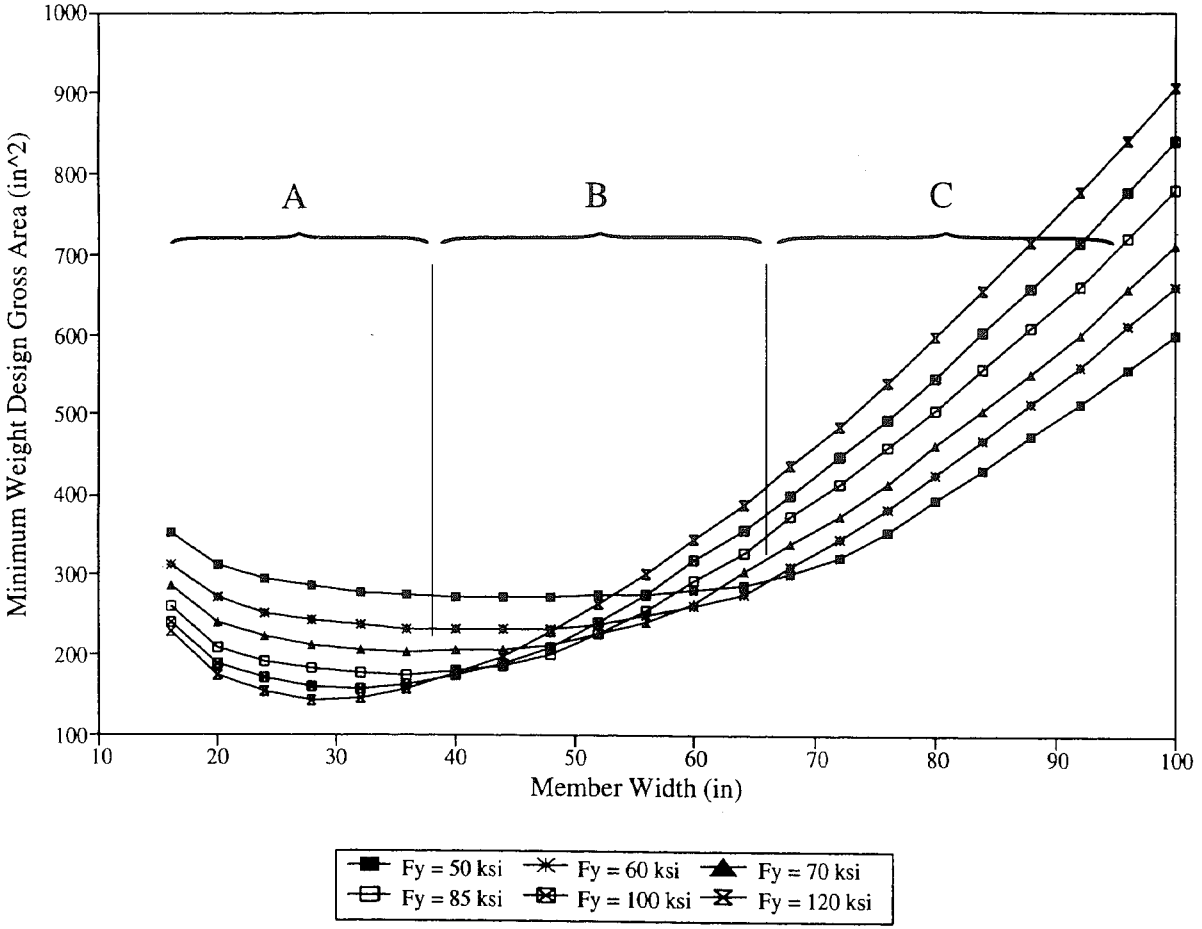

Fig. 6.4-6 Gross Area of Minimum Weight Design Versus Member Width Constraint for Top Chord SU3-SU5

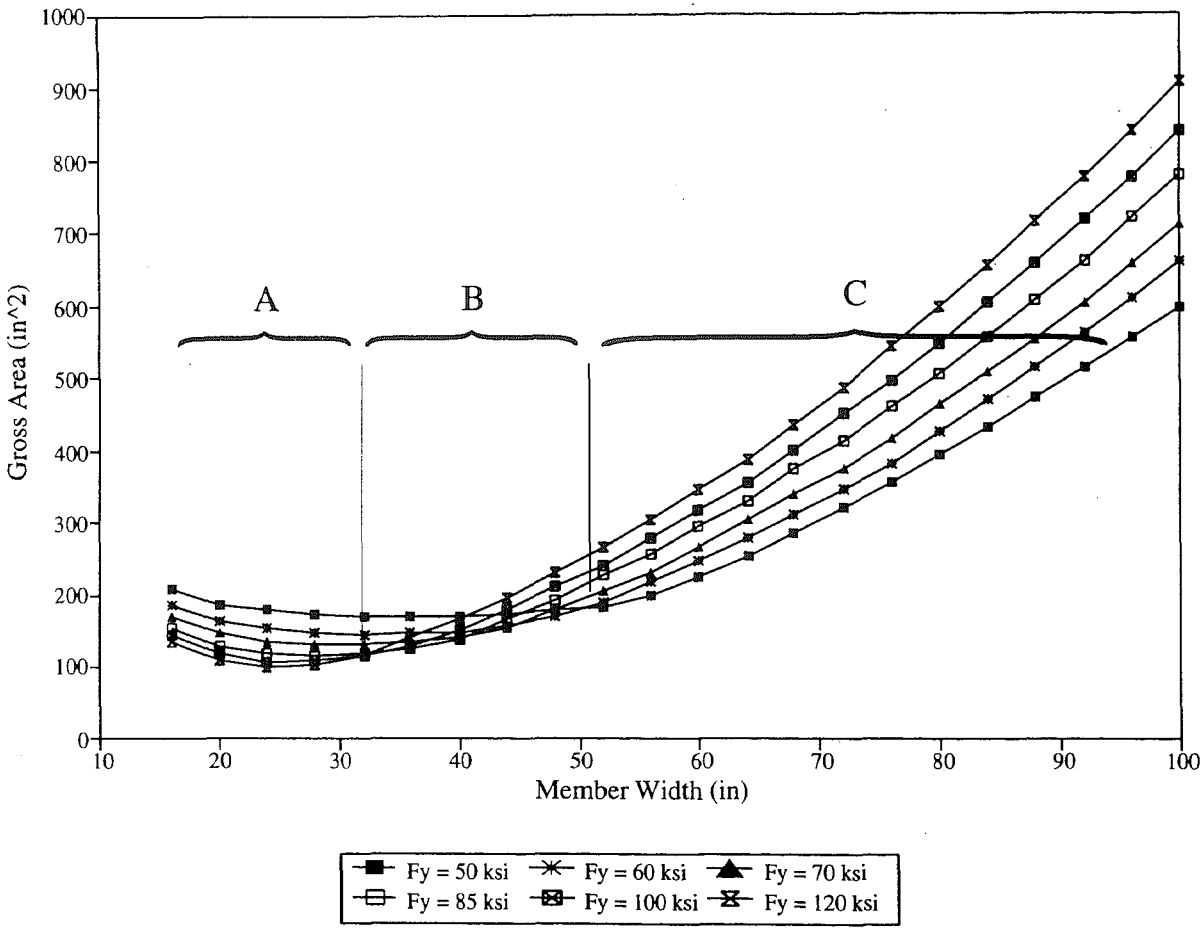

Fig. 6.4-7 Gross Area of Minimum Weight Design Versus Member Width Constraint for Top Chord SU1-SU3

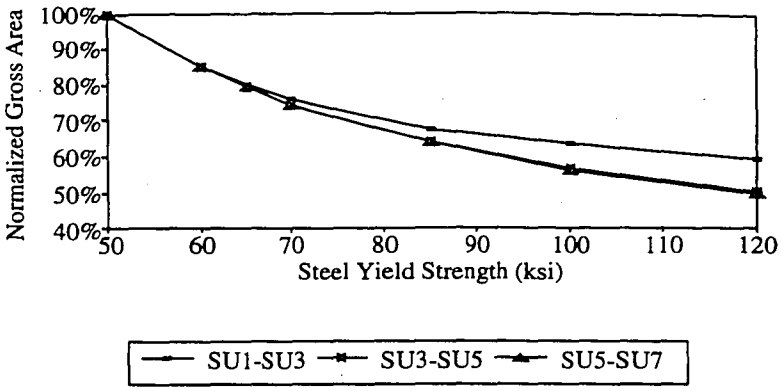

(a) Member Width = 28 in

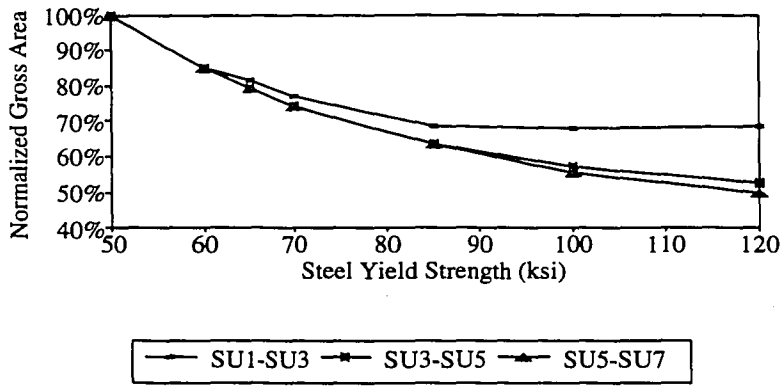

(b) Member Width = 32 in

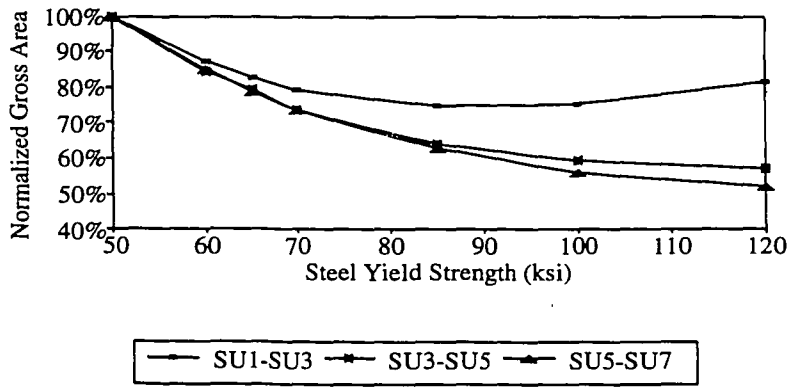

(c) Member Width = 36 in

Fig. 6.4-8 Gross Area of Minimum Weight Design Versus Steel Yield Strength for Members SU1-SU3, SU3-SU5 and SU5-SU7

VITA

The author was born in Changsha, the People's Republic of China on January 2[illegible] 1969. He is the first of two children of Mr. Bi-Hai Li and Mrs. Yu-Rong Liu.

He received his primary education in Changsha, PR China. He was admitted into the No. 1 Middle School of Changsha in 1980 and finished his six years of secondary education in 1986. From September 1987 to July 1992, he studied in Tsinghua University and earned his Bachelor of Engineering Degree in Civil Engineering.

After graduating from college, he went to the Civil Engineering Department of Lehigh University in August 1992 supported by a Graduate School Fellowship Award. From May 1993, he worked as a research assistant on the Federal Highway Administration sponsored project *Innovative Bridge Designs Using Enhanced Performance Steels*, which his thesis research was based on.

END OF TITLE